NASA CR-166,050

NASA Contractor Report 166050

Reliability Analysis and Fault-Tolerant System Development for a Redundant Strapdown Inertial Measurement Unit

Paul Motyka
The Charles Stark Draper Laboratory, Inc.
Cambridge, Massachusetts 02139

Contract NAS1-16887
March 1983

National Aeronautics and
Space Administration

Langley Research Center
Hampton Virginia 23665

NASA Contractor Report 166050

Reliability Analysis and Fault-Tolerant System Development for a Redundant Strapdown Inertial Measurement Unit

Paul Motyka
The Charles Stark Draper Laboratory, Inc.
Cambridge, Massachusetts 02139

Contract NAS1-16887
March 1983

National Aeronautics and
Space Administration

Langley Research Center
Hampton Virginia 23665

TABLE OF CONTENTS

TABLE OF CONTENTS (Continued)

LIST OF ACRONYMS

BITE	built-in test equipment
CSDL	The Charles Stark Draper Laboratory, Inc.
EVT	Edge Vector Test
FDI	failure detection and isolation
GLT	Generalized Likelihood Test
IMU	inertial measurement unit
MTBF	mean time between failures
NASA	National Aeronautics and Space Administration
PFA	Probability of False Alarm
RSDIMU	redundant strapdown inertial measurement unit
SDOF	single degree of freedom
TDOF	two degree of freedom

LIST OF SYMBOLS

A_i, B_i	two input axes of instruments, $i = 1,2,3,4$
b	magnitude of bias failure (rad or m/s)
d	distance from cg to sensor location with components d_x, d_y, d_z (m)
DF_D	failure decision function (rad^2 or (m/s)^2)
DF_{I_J}	failure isolation function for the j^{th} sensor (rad^2 or (m/s)^2)
e_{ij}	edge vectors relating instruments, $i,j = 1,2,3,4$
F_{ij}	logical variables in edge vector algorithm used to detect and isolate failures in instruments i and j, $i,j = 1,2,3,4$
G_ϕ	gravitational constant (9.8062 m/s^2/g (32.1725 ft/s^2/g))
h	altitude (m)
H	sensor configuration geometry matrix
m	sensor outputs (rad or m/s)
n	number of sensors or states
n_x, n_y, n_z	longitudinal, lateral, and normal body-axes linear inertial accelerations (g)
$n_{z_{\eta_i}}, n_{y_{\eta_i}}$	coefficients relating effect of vehicle structural modes on linear accelerations, $i = 1,2,\ldots,6$ (g-s^2)

p, q, r	body axes roll, pitch, yaw rates (deg/s)
$p_{\eta_i}^{\bullet}, q_{\eta_i}^{\bullet}, r_{\eta_i}^{\bullet}$	coefficients relating effect of vehicle structural modes on angular rates, i = 1,2,...,6 (deg)
P	single-step state-transition matrix
P(k,ℓ)	element of matrix P designating the probability that state ℓ makes a transition to state k in a single time step
PDAM	probability of damage
PFiA	probability of an accelerometer failure given that i are in use
PDiA(H,M,S)	probability of detecting an accelerometer failure in the (H = hard, M = mid, S = soft) FDI channel given that i accelerometers are in use.
PIiA(H,M,S)	probability of isolating an accelerometer failure in the H, M, or S FDI channel given that i accelerometers are in use
PFAiA(H,M,S)	probability of an accelerometer false alarm in the H, M, or S FDI channel given that i accelerometers are in use
PFiG	probability of a gyro failure given that i are in use
PDiG(H,M,S)	probability of detecting a gyro failure in the H, M, or S FDI channel given that i gyros are in use
PIiG(H,M,S)	probability of isolating a gyro failure in the H, M, or S FDI channel given that i gyros are in use
PFAiG(H,M,S)	probability of a gyro false alarm in the H, M, or S FDI channel given that i gyros are in use
R_{ij}	edge vector algorithm parity-equation residuals for instruments i and j, i,j = 1,2,3,4 (rad or m/s)
S_i	spin axis of instrument i, i = 1,2,3,4
t	time in seconds (s)

T	failure-detection threshold (rad or m/s for the EVT, rad^2 or $(m/s)^2$ for the GLT)
T_{90}	time for filter to reach 90 percent of its final value (s)
V	(n - 3) × n matrix of parity equations
V_j	j^{th} column of V
x, y, z	body axes system components
x_o	offset of IMU from vehicle centerline (m)
x_s	separation of IMU1, IMU2 from IMU centerline (m)
α	$\frac{\sqrt{3} - 1}{2\sqrt{3}}$
α_{IP}	accelerometer input-pendulous-axes cross-coupling error ($\mu g/g^2$)
β	$\frac{\sqrt{3} + 1}{2\sqrt{3}}$
β_{II}	accelerometer input-axis-squared error ($\mu g/g^2$)
γ	$1/\sqrt{3}$
δ_i	increment of quantity i
$\delta(t)$	state probability vector
ε	scale-factor error (ppm)
ζ	measurement noise which is Gaussian with zero mean
η_i	generalized bending mode coefficients, i = 1,2,...,6
λ	bias error (deg/s or μg)
μ	misalignment error (rad)
ρ	GLT parity-equation residuals (rad or m/s)
σ	standard deviation of the instrument noise (rad or m/s)
ω	three-dimensional vector of body-axes inertial linear accelerations (g) or angular rates (deg/s)

ω^{B}_{ij}	body axes component of the output of the i^{th} accelerometer or gyro along j^{th} axes (m/s or rad)

Subscripts

A1, B1	sensor input axes
a	accelerometer
B	structural mode effects included
cg	center of gravity
F	presence of failed sensor
f	filtered
i,j,k,ℓ	element number, row, and/or column
L	left
ℓa	lever arm
m	positive maximum or upper bound
N	absence of failed sensor
R	right
2	2 Hz
50	50 Hz

Superscripts

B	body-axes system
N	number of time steps in a time interval
P	pendulous-axes system
T	transpose
^	estimate

SECTION 1

INTRODUCTION

The material contained in this report is a result of the study of the Redundant Strapdown Inertial Measurement Unit (RSDIMU) being developed and evaluated by the NASA Langley Research Center. The work was conducted by The Charles Stark Draper Laboratory, Inc. (CSDL) under NASA Contract NAS1-16887 entitled the False Alarm/Reliability Analyses for a Separated Dual-Fail Operational Redundant Strapdown Inertial Measurement Unit. It is a follow-on to a previous effort described in Reference 1. The goal of the initial effort was to assess the feasibility of performing failure detection and isolation (FDI) for the RSDIMU in an air transport environment, develop and evaluate FDI algorithms for the RSDIMU, and analyze FDI system performance.

The present study uses the results of the previous effort as a basis. The RSDIMU sensor configuration, a description of some of the basic concepts associated with FDI and a summary of the major results of the previous study are presented in Section 2 to provide the reader with some background into the system being analyzed and concepts being evaluated.

One of the major reasons for considering the dual, separated RSDIMU is to improve the survivability of the aircraft when damage to the inertial measurement unit occurs, while achieving a desired level of fault tolerance with fewer instruments. This subject is addressed in Section 3 where a methodology for quantitatively analyzing the reliability of redundant avionics systems in general and the dual, separated RSDIMU system in particular is developed and applied. A Markov model reliability

analysis tool is developed and applied. The results of the parametric study of significant instrument and FDI system variables are presented and discussed.

The detection and isolation of failures of the dual, separated RSDIMU is accomplished by comparing a function of the sensor outputs with a threshold. The thresholds for a colocated cluster of instruments must account for the nominal sensor errors and aircraft dynamic environment to detect the smallest possible level of failure without encountering a prohibitive number of false alarms or the false detection of failures. The separation of the RSDIMU into two separated clusters severely complicates the selection of the thresholds. The incremental structural mode and accelerometer lever arm effects between the locations of the two instrument clusters must now be taken into account. A technique is developed and analyzed for generating the thresholds for a dual, separated RSDIMU taking all of the previously mentioned factors into account. Special emphasis is given to the detection of multiple, nonconcurrent failures. Section 4 contains the results.

Section 5 summarizes the results of this study.

Dr. P. Motyka was the project leader for CSDL while Dr. J. Lee developed and exercised the RSDIMU Markov model discussed in Section 3.

SECTION 2

BACKGROUND AND RESULTS OF THE PREVIOUS STUDY

2.1 Sensor Configuration

The inertial measurement unit shown in Figure 1 is a redundant strapdown package employing four two-degree-of-freedom (TDOF) gyros (accelerometers) in a semi-octahedral geometry. The instruments are positioned such that the spin (pendulous) axes are normal to the four faces of the semi-octahedron and point out. The two measurement axes of the gyros and accelerometers lie in the plane of the face and are symmetric about the face centerline. The RSDIMU consists of two separate packages (faces 1 and 2, faces 3 and 4) which may be spatially separated along a track in the lateral direction. Thus, it may be treated as two tetradic IMUs as indicated in Figure 2. The reason for separating the RSDIMU into two halves is to provide protection against damage effects due to lightning, structural failure, etc. The benefits of redundancy in the form of improved system reliability are retained by using sensor information from both halves of the IMU for failure detection and isolation purposes.

The nominal geometry matrix, defining the sensor input axes relative to the vehicle body axes is

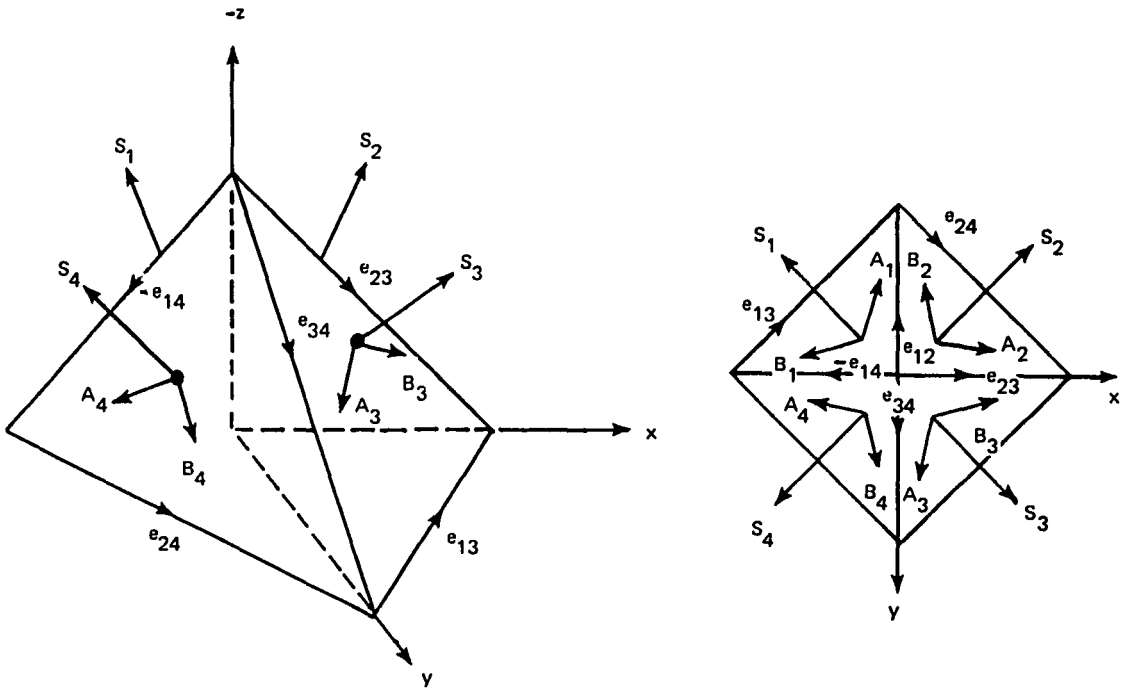

Figure 1. RSDIMU instrument geometry.

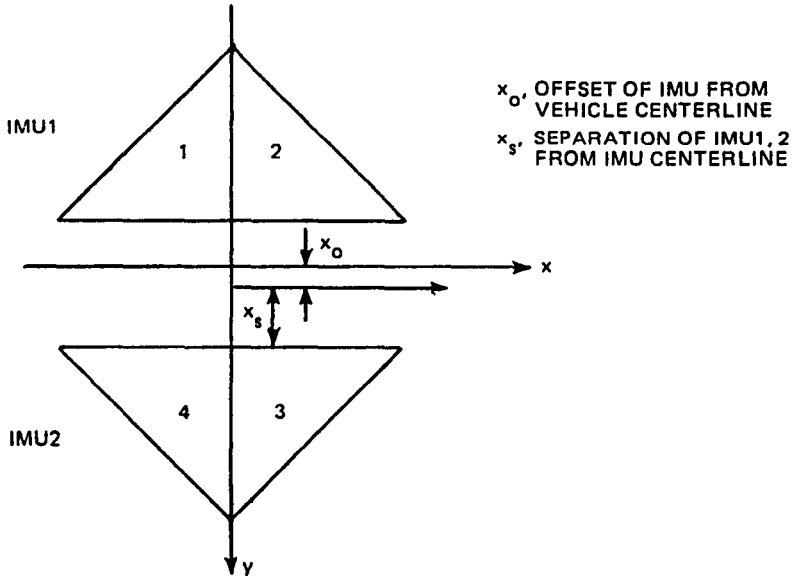

Figure 2. Separation of sensor configuration into two IMUs.

$$H = \begin{bmatrix} \alpha & -\beta & \gamma \\ -\beta & \alpha & \gamma \\ \beta & \alpha & \gamma \\ -\alpha & -\beta & \gamma \\ \hline -\alpha & \beta & \gamma \\ \beta & -\alpha & \gamma \\ -\beta & -\alpha & \gamma \\ \alpha & \beta & \gamma \end{bmatrix}$$

where

$$\alpha = \frac{\sqrt{3} - 1}{2\sqrt{3}}$$

$$\beta = \frac{\sqrt{3} + 1}{2\sqrt{3}}$$

$$\gamma = \frac{1}{\sqrt{3}}$$

The dashed line indicates the separation of the RSDIMU into two halves.

2.2 General Concepts of FDI

This section is included to provide the reader with a background in the general concepts applied to detect and isolate sensor failures. It will allow a greater understanding and appreciation of the material presented in the following sections of the report.

In order to detect and isolate sensor failures, a system of parity equations is solved. Parity equations are linear combinations of the sensor outputs selected to enhance the uncertainties (failures) associated with the sensors. Furthermore, the effects of the quantity which the instruments measure, i.e., the angular rates or linear accelerations, are removed from consideration by the parity equations.

Failure detection occurs as a result of comparing the parity equation residuals or a function of them to a threshold. If the threshold is exceeded, a failure is declared and the failure is then isolated. Failure isolation is accomplished using the parity equation residuals. Several methods are used depending upon the algorithm employed. Logical operations based on the residuals which exceed the threshold is one technique used, e.g., a combination of residuals exceeding the thresholds indicates the failure of a particular sensor. Another approach involves the dot product of the vector of parity equation residuals with vectors defined by the coefficients of the parity equations to isolate a failure.

This, in essence, is the methodology applied to detect and isolate sensor failures. However, complications arise when applied to a practical situation. For example, the parity equation residuals are ideally zero when a failure is not present and nonzero when a failure has occurred. In reality, the residuals are nonzero because of the uncertainties associated with the sensors, i.e., the sensor errors, sensor noise, structural mode effects, accelerometer lever-arm effects, etc. The residuals due to these factors dictate the level of failure which can be detected since they do not arise from failures and are a result of normal, although undesirable, sensor behavior. In a dynamic environment these uncertainties may be executed to a greater degree. To avoid the false detection of failures, i.e., false alarms, the thresholds may have to be compensated for this effect. One possible approach to handling this problem is the use of dynamic thresholds which are a function of the environment. Another is in-flight identification and compensation of the sensor error effects in the FDI decision process.

Normally, unfiltered sensor data is used to detect and isolate sensor failures of a large magnitude since it is desired to remove their effects before they affect the controllability of the vehicle. Another factor in the design of FDI systems is that the effects of small magnitude failures may be masked by the instrument uncertainty effects. Filtering of the parity equation residuals may have to be introduced into

the FDI system to enhance their detectability. This is at the expense of a longer detection time and a design tradeoff exists. The presence of several channels in the FDI system to detect and isolate different levels of failures may result.

Two FDI algorithms have been investigated during the course of this study; the Edge Vector Test (EVT) and the Generalized Likelihood Test (GLT). They will be defined later in the report when it becomes expeditious to do so.

2.3 Summary of the Previous Study

As mentioned previously, this effort is a follow-on to a previous study. During the initial study, the feasibility of performing FDI for the RSDIMU in an air transport environment was demonstrated and a methodology was developed for the design and evaluation of fault-tolerant systems. A spectrum of failure magnitudes was accounted for. The RSDIMU was also used for both flight control and navigation purposes during this study. The GLT and EVT FDI algorithms were compared with respect to factors such as the parity equations used, software requirements, failure detection and isolation capability, thresholds, etc. The GLT algorithm is preferred because of its technical maturity. It was also determined that dynamic thresholds were needed for the soft failure channel and an algorithm developed for generating them.

The block diagram of the FDI system which evolved from this study is shown in Figure 3. This system reflects the ideas and conclusions addressed in the previous paragraphs and will be used as the basis for the technical development in the succeeding sections.

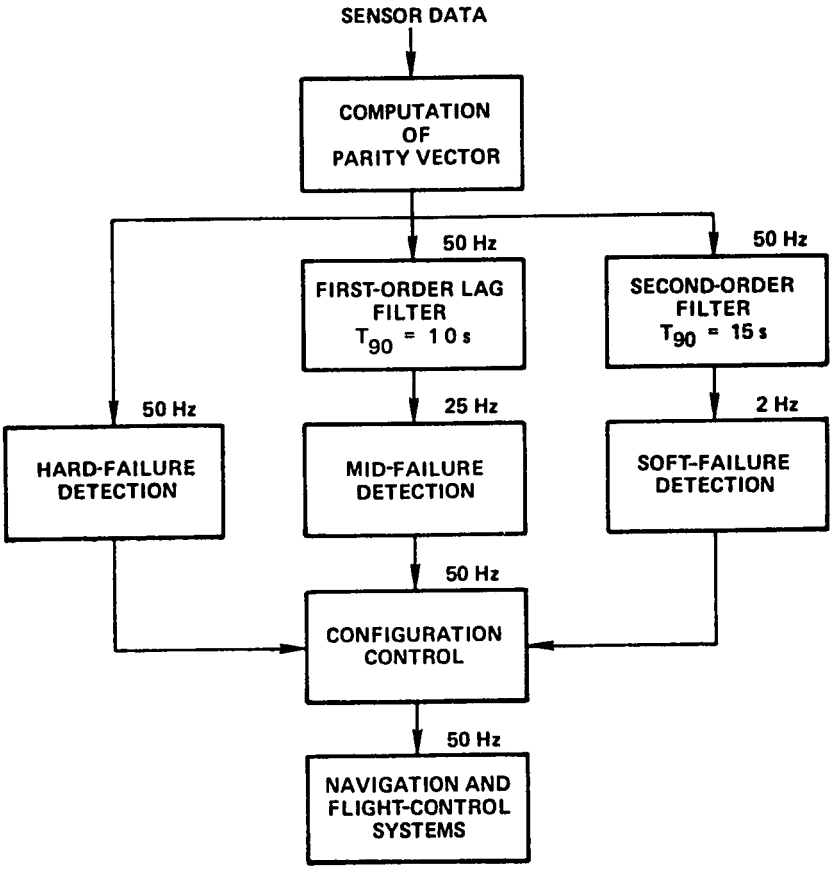

Figure 3. FDI algorithm block diagram.

SECTION 3

RSDIMU RELIABILITY ANALYSIS

3.1 Introduction

The goal of this section is to develop and apply a methodology for quantitatively analyzing the reliability of redundant avionics systems in general and the dual, separated RSDIMU system in particular.

The need for an analytic reliability evaluation tool to evaluate the performance of fault-tolerant systems is clear. Evaluation of these systems by testing is prohibitive since their highly reliable nature implies a large number of test samples and/or extremely long test periods. In addition, the probabilistic nature of fault-tolerant systems precludes application of conventional analysis techniques such as covariance analysis.

CSDL's approach to this problem is to apply a Markov reliability evaluation model, defined in terms of the operational states of the system, to predict system performance through figures-of-merit. This methodology has been developed and refined during the course of several technological development programs. It can be used to obtain quantitative data to support the specification and validation of requirements, architecture evaluation, the cross comparison of systems, design tradeoffs, and the efficient allocation of resources throughout the definition, design, and test phases of their development. The Markov model is defined in terms of states which represent the operational modes of the system. These include not only the normal mode of system operation with no failed

components present but the degraded modes as well which represent the state of system operation arrived at because of correct or incorrect decisions made by the redundancy management system, e.g., the detection and isolation of failures, false alarms, missed detections, etc. In this sense, the model is defined to truly represent the operation of the fault-tolerant system. The Markov model is used to generate the probability of the system being in one of the defined operational states after a prespecified length of time using the single-step state-transition probabilities.

Different measures of system performance are obtained from the Markov model approach. One of the most important and widely used is the probability of the system becoming inoperative by the end of the mission. Other outputs which can be obtained are the time histories of the state probabilities, the state occupancy statistics, and the mean and variance of the time to system failure.

3.2 Description of Procedure

The Markov model evolves from a system block diagram outlining the partitioning of the system and the interconnections among the various system components. This block diagram is then used to define the system's operational states. A significant problem in developing a Markov model lies in determining the states that are sufficient to characterize the operation of the system while at the same time limiting their number and, hence, the order of the system for computational reasons. The order of the Markov model grows exponentially as a function of the number of states.

The next step in the procedure is to develop single-step state-transition diagrams. These diagrams indicate the states that may evolve from a given initial state in a single step, the decisions made in achieving these states, and the probabilities associated with these decisions. The state-transition probabilities are then calculated from

the state-transition diagram and put into matrix form for Markov probability theory application. Each element of the state-transition matrix is the probability of going from an initial state to another state in a single time step.

The last step in the procedure involves the propagation in time of the system probabilities by raising the matrix of transition probabilities to a power equal to the number of time steps. Auxiliary statistical information regarding the performance of the FDI system is also calculated.

3.3 Summary of Equations

Let P represent the single-step state-transition matrix of the Markov model. The element $P(k,\ell)$ of P designates the probability that state ℓ makes a transition to state k in a single time step. The states are ordered in such a way that transitions from any state ℓ to any state k where $k < \ell$ is impossible. This is equivalent to assuming that the failures and FDI decisions are irreversible. P is a lower triangular square matrix with its dimension equal to the number of states, n. Let $\delta(t)$ represent the n-dimensional state probability vector for the system. The following relations must hold for the columns of P and for $\delta(t)$

$$\sum_{k=1}^{n} P(k,\ell) = 1.0 \text{ for } \ell = 1,\ldots,n$$

$$\sum_{\ell=1}^{n} \delta_{\ell}(t) = 1.0 \text{ for all } t$$

These relations reflect the requirement that each state must undergo a transition to some state (perhaps itself) in each time step, and that the system must be in one of the n states of the model at all times.

Assuming that the probabilities which define the elements of the matrix P are invariant in time, the state probability vector $\delta(t)$ at any time t can be computed by

$$\delta(t) = P^N \delta(0)$$

where the exponent N designates the number of time steps in an interval of length t. The matrix P^N is referred to as the N-step transition probability matrix. The individual columns of P^N thus correspond to the state probability vectors $\delta_\ell(t)$ given that the system was initialized to state ℓ.

3.4 Definition of the RSDIMU Operational States

The RSDIMU system block diagram, shown in Figure 4, forms the basis for the discussion regarding the definition of the operational states for the reliability model presented in Table 1. This diagram indicates the system components, their level of redundancy, and their interconnections. The manner in which the RSDIMU is separated into two halves is also apparent from this diagram.

The operational states of the RSDIMU have been defined to reflect failures of the sensors only and the FDI system decisions made with regard to them. The impact of failures of the computers and additional peripheral equipment on system reliability has been neglected during this study. However, there is no reason why the reliability analysis could not be modified to reflect these additional components. The effects of damage have been considered.

27 states have been defined for the RSDIMU Markov model. The means by which some of the states are arrived at is discussed to give the reader insight into the reasons for their being defined. The first state is the assumed starting condition for system operation where no sensor failures are present. States 2 through 25 reflect various stages of

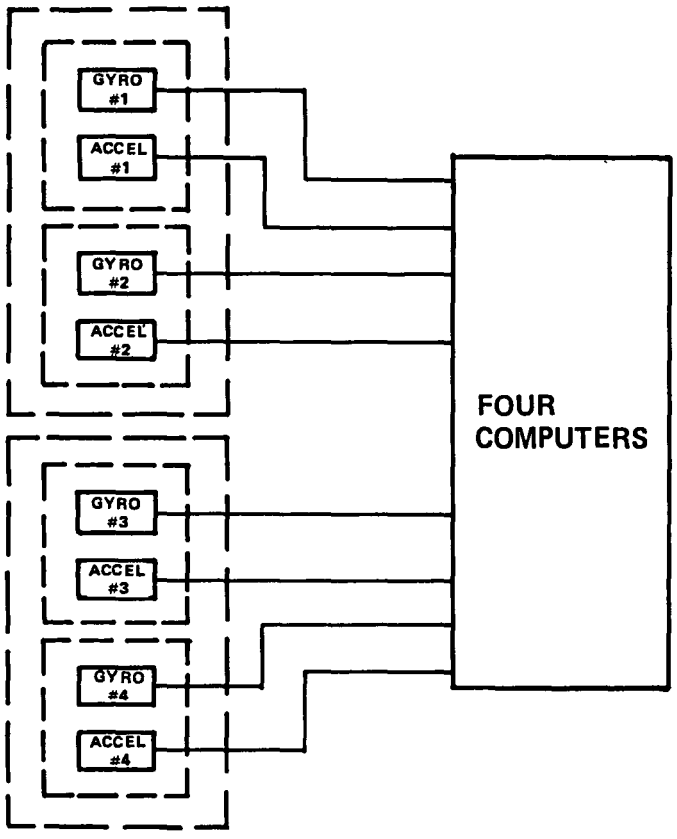

Figure 4. RSDIMU system configuration.

degraded RSDIMU system operation due to the effects of sensor failures and the FDI system decisions made during the course of system operation. For example, State 2 represents the condition where a sensor has failed but the failure has not yet been detected by the FDI system. State 3 defines the operational mode where either the failure present in State 2 has been detected and correctly isolated and the system reconfigured to remove its effects, a gyro false alarm has occurred when the system was initially in State 1 and an unfailed sensor removed from operation, or a gyro failure occurs while in State 1 and it is detected and correctly isolated.

Table 1. Definition of RSDIMU Operational States.

State	Definition
1	4 Gyros in Use, 4 Good; 4 Accelerometers in Use, 4 Good
2	4 Gyros in Use, 3 Good, 1 Failed; 4 Accelerometers in Use, 4 Good
3	3 Gyros in Use, 3 Good; 4 Accelerometers in Use, 4 Good
4	4 Gyros in Use, 4 Good; 4 Accelerometers in Use, 3 Good, 1 Failed
5	4 Gyros in Use, 4 Good; 3 Accelerometers in Use, 3 Good
6	4 Gyros in Use, 3 Good, 1 Failed; 4 Accelerometers in Use, 3 Good, 1 Failed
7	4 Gyros in Use, 3 Good, 1 Failed; 3 Accelerometers in Use, 3 Good
8	3 Gyros in Use, 3 Good; 4 Accelerometers in Use, 3 Good, 1 Failed
9	3 Gyros in Use, 3 Good; 3 Accelerometers in Use, 3 Good
10	3 Gyros in Use, 2 Good, 1 Failed; 4 Accelerometers in Use, 4 Good
11	2 Gyros in Use, 2 Good; 4 Accelerometers in Use, 4 Good
12	4 Gyros in Use, 4 Good; 3 Accelerometers in Use, 2 Good, 1 Failed
13	4 Gyros in Use, 4 Good; 2 Accelerometers in Use, 2 Good
14	3 Gyros in Use, 2 Good, 1 Failed; 4 Accelerometers in Use, 3 Good, 1 Failed

Table 1. Definition of RSDIMU Operational States (cont).

State	Definition
15	3 Gyros in Use, 2 Good, 1 Failed; 3 Accelerometers in Use, 3 Good
16	2 Gyros in Use, 2 Good; 4 Accelerometers in Use, 3 Good, 1 Failed
17	2 Gyros in Use, 2 Good; 3 Accelerometers in Use, 3 Good
18	4 Gyros in Use, 3 Good, 1 Failed; 3 Accelerometers in Use, 2 Good, 1 Failed
19	3 Gyros in Use, 3 Good; 3 Accelerometers in Use, 2 Good, 1 Failed
20	4 Gyros in Use, 3 Good, 1 Failed; 2 Accelerometers in Use, 2 Good
21	3 Gyros in Use, 3 Good; 2 Accelerometers in Use, 2 Good
22	3 Gyros in Use, 2 Good, 1 Failed; 3 Accelerometers in Use, 2 Good, 1 Failed
23	3 Gyros in Use, 2 Good, 1 Failed; 2 Accelerometers in Use, 2 Good
24	2 Gyros in Use, 2 Good; 3 Accelerometers in Use, 2 Good, 1 Failed
25	2 Gyros in Use, 2 Good; 2 Accelerometers in Use, 2 Good
26	Same as 25, but RSDIMU damaged
27	Failed State

States 4 and 5 are similar to States 2 and 3 except that accelerometer failures are present rather than gyro failures. The occurrence of a gyro failure when an accelerometer failure exists and vice versa leads to the definition of State 6 as one of the possible modes of RSDIMU operation. State 7 results from any one of four events; the detection and isolation of the accelerometer failure present in State 6, an undetected gyro failure when the system is operating in State 5, or an accelerometer false alarm or failure which is detected and correctly isolated when the system is in State 2.

The rest of the Markov model states through 25 evolve as a result of similar thinking as more sensor failures and FDI decisions are made during the course of operation of the RSDIMU system. Eventually, a mode of operation results for which two unfailed gyros and two unfailed accelerometers are available for use. This is State 25. The only other states that require elaboration are States 26 and 27. State 26, although similar to State 25, differs from it in that it arises as a result of damage effects to the RSDIMU. It is defined separately should it be desired to assess the impact of damage effects independently of the normal mode of system operation. The last state of the model is defined as the failed state, State 27, which includes modes of operation for which there are fewer than two unfailed gyros or two unfailed accelerometers available, either because of damage effects or sensor failures or the presence of two failed gyros or two failed accelerometers simultaneously.

The question naturally arises concerning the definition of a suitable and valid figure-of-merit for assessing the reliability performance of the RSDIMU system. The measure selected is the probability of having a failure present in the system. It includes the probability of the system being in any one of the states listed in Table 2. This parameter was chosen to assess system performance since it covers all ranges of FDI system performance. For example, if the FDI system is perfectly designed, all of the instrument failures will be detected and correctly

Table 2. States defining system failure.

State	Failure Present	
	Gyro	Accel
2	✓	
4		✓
6	✓	✓
7	✓	
8		✓
10	✓	
12		✓
14	✓	✓
15	✓	
16		✓
18	✓	✓
19		✓
20	✓	
22	✓	✓
23	✓	
24		✓
27	✓	✓

isolated and the probability of being in State 27 will be the measure of the reliability of the system. However, if the performance of the FDI system is poor, failures will not be detected and isolated as quickly or as correctly and the probability of being in the intermediate states will more aptly define system performance. Any system for which a failure is present is detrimental to achieving the goals of the system and the definition of the probability of having a failure present in the system as a figure-of-merit covers all extremes of system operation and performance.

3.5 State Transition Diagrams

The next step in the development of the RSDIMU Markov reliability model involves the generation of the state transition diagrams. These diagrams indicate the effects of component failures, the FDI system decisions, and the operational states which result from them given an initial starting state. As an example, Figure 5 shows the transitions out of the initial state of RSDIMU system operation for all possible component failures, all possible FDI decisions, and the effects of damage. The final state of operation which results from each of these factors is also indicated. The state transition diagrams also reflect the basic structure of the FDI system presented in Figure 3 in that three channels of operation have been defined to cover hard, medium, and soft failures.

Once generated, the state transition diagrams are used to generate the state transition probabilities or elements of the single-step state transition matrix. This is done by multiplying the entries along a given path to obtain the conditional probability of transitioning to the end state in a single time step given operation in the initial state.

3.6 Additional Markov Model Assumptions and Considerations

The state transition probabilities for the RSDIMU reflect the fact that the three channels of FDI system operation are performed at different rates. This is done by assuming that the Markov model is run

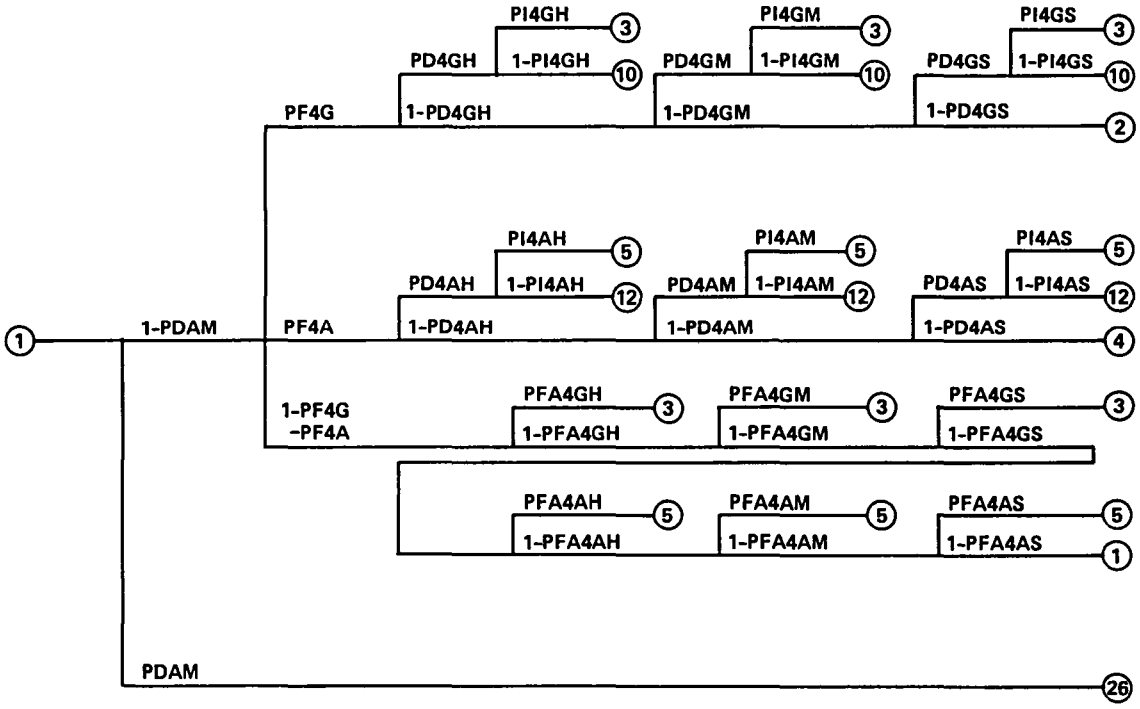

Figure 5. RSDIMU state transition diagram.

at the lowest FDI system frequency, i.e., that of the soft-failure channel, and modifying the probabilities associated with the hard- and mid-failure channels to account for the higher frequency of operation. For example, the accelerometer hard-failure channel probabilities are modified as follows to reflect the fact that it operates at a frequency which is 25 times faster than that of the soft-failure channel.

$$PD4AH_2 = 1.0 - (1.0 - PD4AH_{50})^{25}$$

$$PI4AH_2 = 1.0 - (1.0 - PI4AH_{50})^{25}$$

$$PFA4AH_2 = 1.0 - (1.0 - PFA4AH_{50})^{25}$$

The Markov model probabilities must also reflect any effects of IMU separation and communication between the two halves of the system. Communication allows treating the dual, separated system as a single cluster of instruments for FDI purposes. That is, information from both halves can be used to detect and isolate failures. The FDI system thresholds must also account for separation effects. They must be selected to account for instrument uncertainties such as sensor errors, sensed structural mode effects, and accelerometer lever-arm effects, to avoid the detrimental effects of false alarms. The state transition probabilities must then reflect the FDI system probabilities which result from the selection of the thresholds to account for these factors.

Another assumption that could have been made during the development of the Markov model for the RSDIMU but was not is that if a failure is not detected and/or isolated after a specified number of time steps, the system is in the failed state. As the present Markov model is defined, a failure can be detected and/or isolated continuously after its occurrence until the mission terminates.

3.7 Nominal Markov Model Parameters

The nominal parameters selected for evaluating the reliability of the RSDIMU via the Markov model are listed in Table 3. A system with perfect FDI has been assumed, i.e., a probability of 1.0 for detection and correct failure isolation and zero probability of false alarm. The MTBF of the gyro is 13,333 hours and that of the accelerometers is 16,666 hours. These numbers were obtained from Reference 2. A mission time of 1 hour and zero probability of damage effects have been assumed. The nominal data rates for the three FDI system channels are also listed.

3.8 Results

A large number of Markov model computer runs were made to assess the effects of different system parameters on the reliability of the RSDIMU. Two baseline values of reliability were obtained. One is

Table 3. Markov model nominal parameters.

Parameter	Units	Value
Levels of FDI	-	3.
Hard Channel Data Rate	Hz	50.
Mid Channel Data Rate	Hz	25.
Soft Channel Data Rate	Hz	2.
Mission Time	Hours	1.
Gyro Failure Rate	$/10^6$ Hours	76.
Accelerometer Failure Rate	$/10^6$ Hours	59.
Probability of Failure Detection	-	1.0
Probability of Correct Failure Isolation	-	1.0
Probability of False Alarm	-	0.0
Probability of Damage Effects	-	0.0

2.576×10^{-12} which is the probability of system failure for the nominal Markov model parameters presented in Table 3. The other baseline value is 5.397×10^{-4} which is the probability of system failure with no FDI and redundancy management present. Thus, an eight order of magnitude improvement in RSDIMU reliability can be obtained under optimum conditions.

Other RSDIMU reliability results are graphically presented in Figures 6 through 12. Figure 6 shows the effect of gyro failure rate on the probability of RSDIMU system failure. The results indicate that if the reliability of one of the instruments is much worse than that of the other, that instrument will govern the reliability of the RSDIMU. Conversely, little improvement in system reliability can be achieved by improving the reliability of the more reliable instrument.

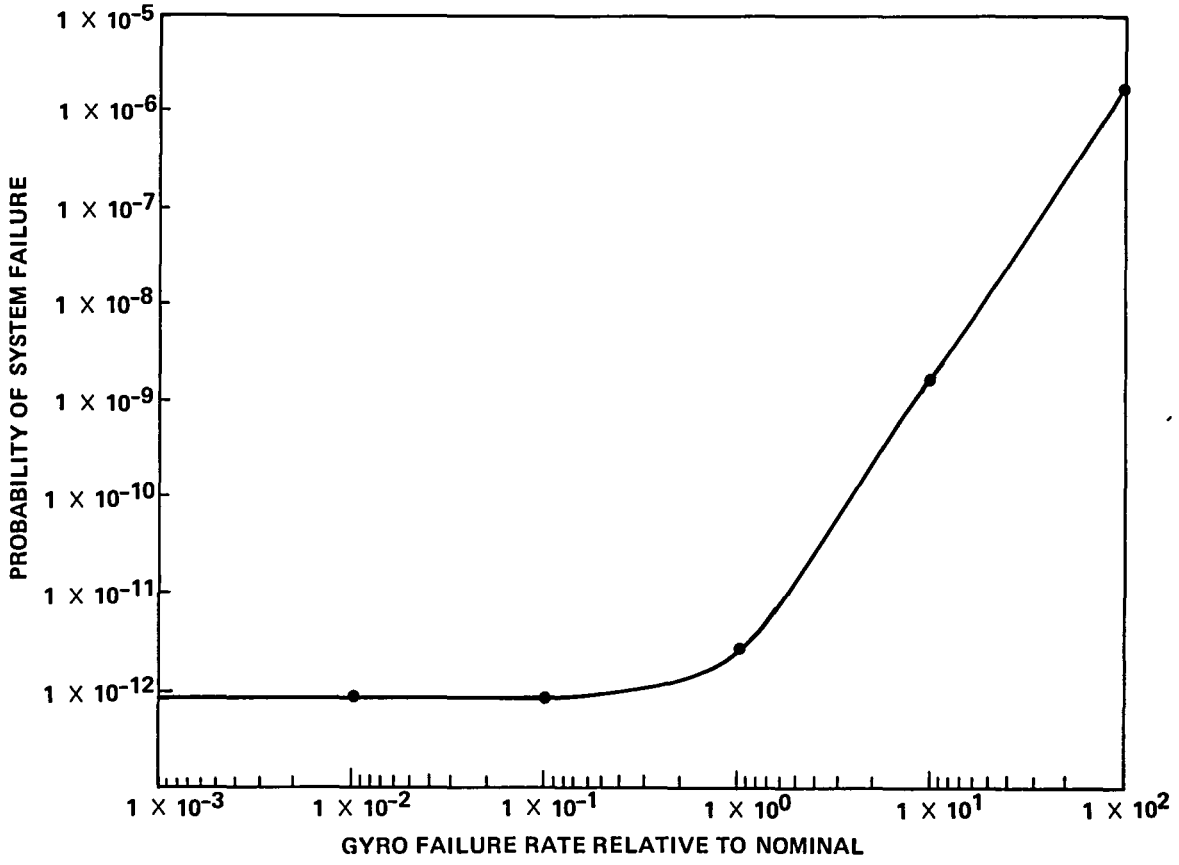

Figure 6. Probability of system failure vs. gyro failure rate.

The effect of varying the failure rates of both the gyros and accelerometers together on the RSDIMU system reliability is shown in Figure 7. The reliability of the RSDIMU improves three orders of magnitude for each order of magnitude improvement in the reliability of the gyros and accelerometers.

The impact of false alarms on RSDIMU reliability is indicated in Figure 8. Their effect is dependent upon the level of FDI system thresholds selected, thus the independent variable in this study is the level of thresholds relative to the instrument noise level. Per sample values of the probability of false alarm (PFA) can be calculated making certain assumptions. If the GLT method of FDI is assumed, the probability of

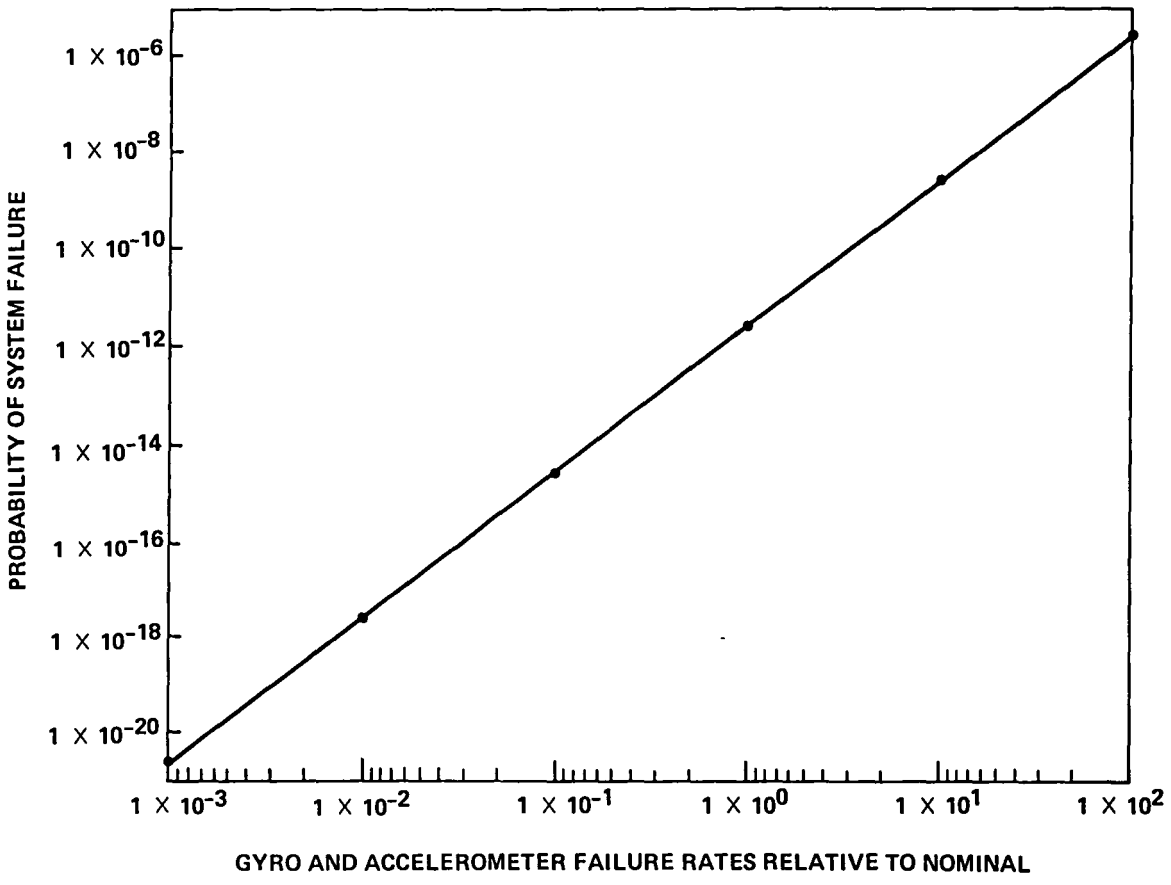

Figure 7. Probability of system failure vs. gyro and accelerometer failure rates.

false alarm can be calculated from an χ^2 probability density function with n - 3 degrees of freedom (Reference 3). The resultant values of PFA are presented in Table 4. The results of this study indicate that a threshold level of 7.5σ or greater will minimize the impact of false alarms on RSDIMU system reliability.

The next factor considered in the study was the probability of failure detection for the soft-failure FDI system channel. The results of the parametric study of this variable are presented in Figure 9. They indicate that a significant improvement in system reliability is

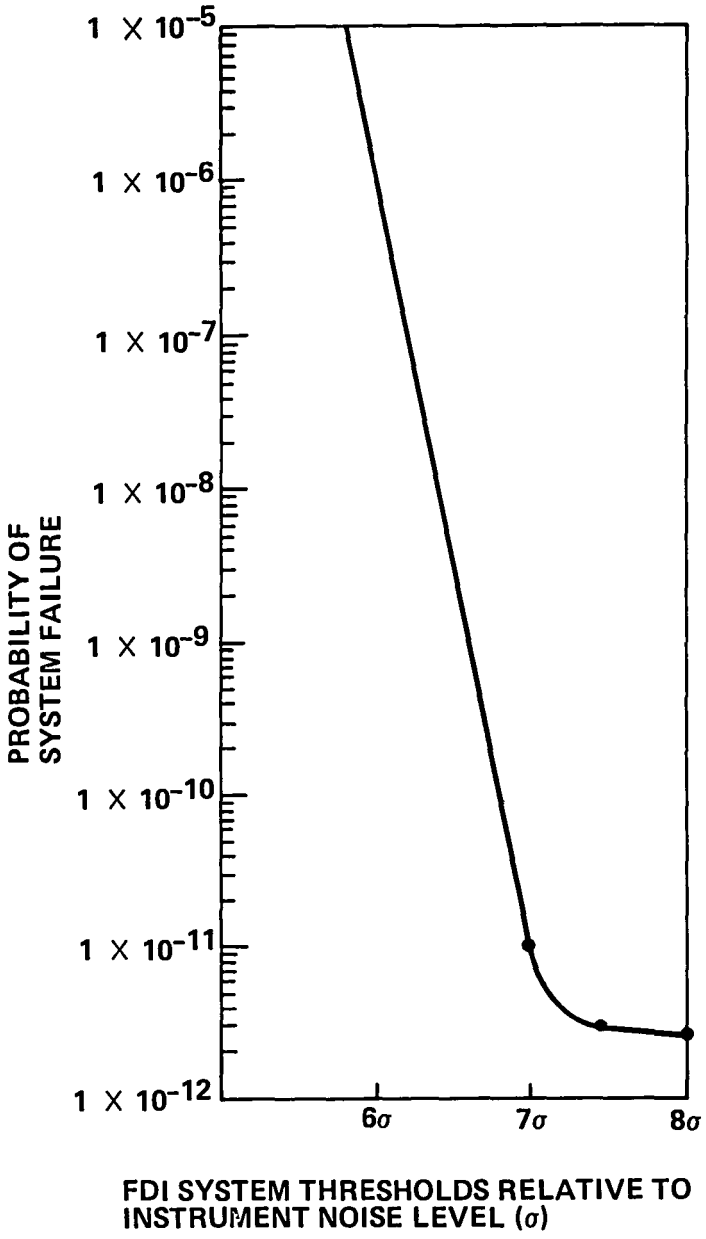

Figure 8. Probability of system failure vs. FDI system threholds

Table 4. Probability of false alarm for the RSDIMU Markov model reliability study.

Threshold (σ)	Number of Instruments		
	4	3	2
6	9.50×10^{-7}	7.49×10^{-8}	1.97×10^{-9}
7	2.22×10^{-9}	1.30×10^{-10}	2.56×10^{-12}
7.5	7.08×10^{-11}	3.16×10^{-12}	7.08×10^{-14}
8	1.81×10^{-12}	8.21×10^{-14}	1.25×10^{-15}

achieved by incorporating some fault tolerance into the RSDIMU system. On the other hand, the achievement of the maximum improvement in system reliability requires the detection of virtually all failures encountered. Multiple FDI channels can help significantly in this regard because if a failure is not detected by one channel, it is a virtual certainty that it will be detected by the channel in the hierarchy with the next smallest thresholds. Typical values of the probability of detection, including self-test, run in the vicinity of 0.8 to 0.9.

The previous results apply to the soft-failure channel. Parametric studies were also made of the mid-failure channel probability of detection with the soft-failure channel probability of detection equal to 1.0 because of the lower thresholds, and similarly for the hard-failure channel. These results coincided with the value for the baseline case with perfect FDI for all cases. This conclusion is a consequence of the fact that a failure can be detected from its occurrence until the end of the mission. If enough samples are taken, the probability of detecting the failure will eventually reach unity and perfect FDI will be achieved.

Figure 10 presents the effect of the probability of correct isolation for the soft-failure channel on RSDIMU system reliability. The

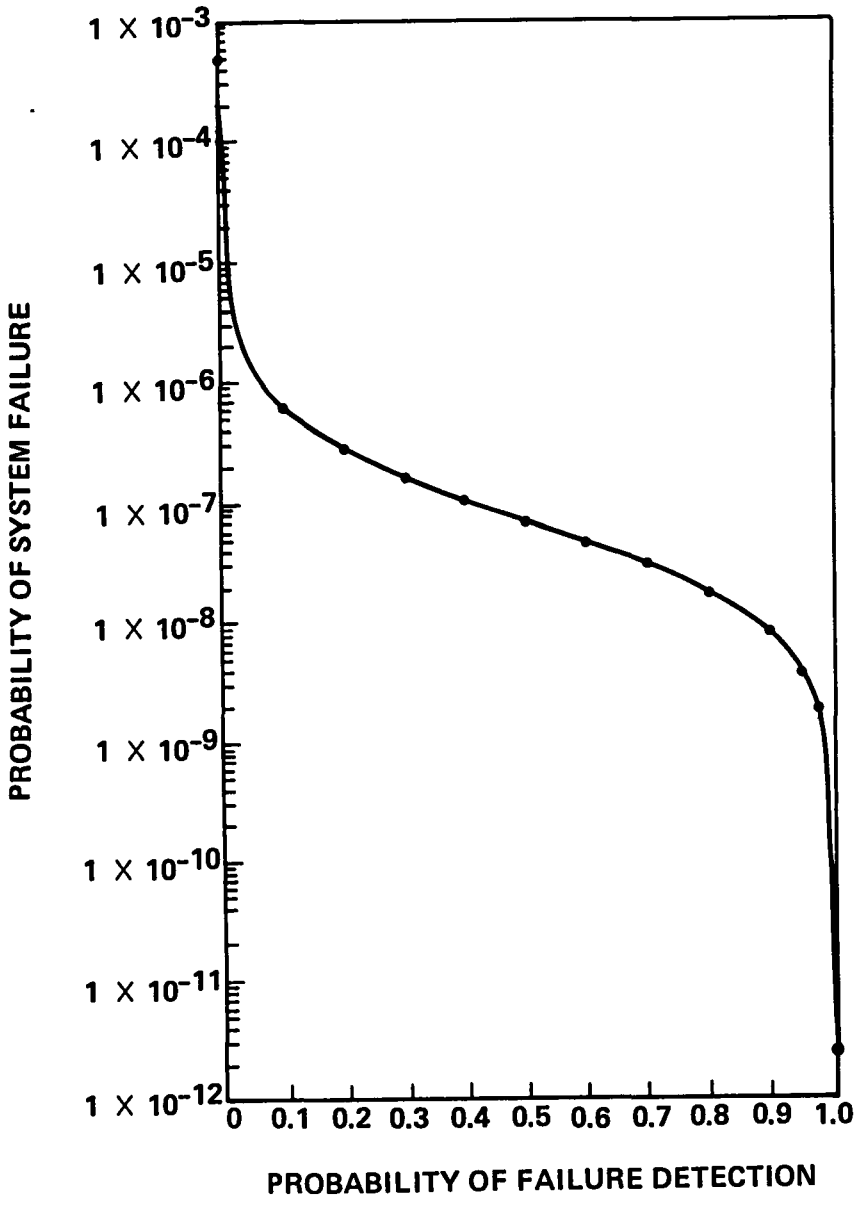

Figure 9. Probability of system failure vs. probability of failure detection for a single FDI system channel.

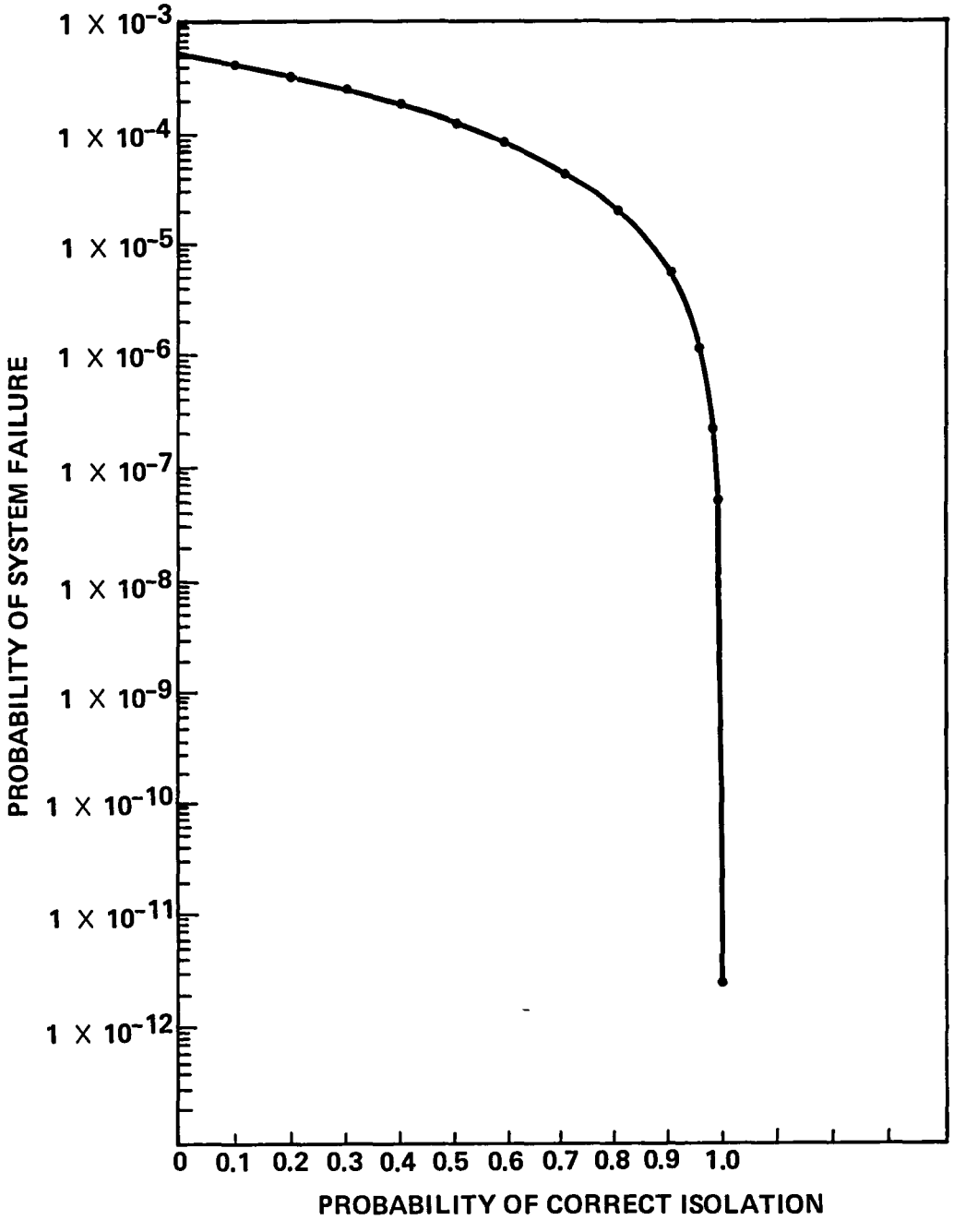

Figure 10. Probability of system failure vs. probability of correct isolation for a single FDI system channel.

results indicate that correct failure isolation is a must to obtain the maximum improvement in system reliability. Otherwise, an instrument failure is present which is defined as a system failure.

The probability of damage is addressed in Figure 11. On the average, an improvement of three orders of magnitude in system reliability for a one-hour mission is achieved because of the separation of the IMU into two units.

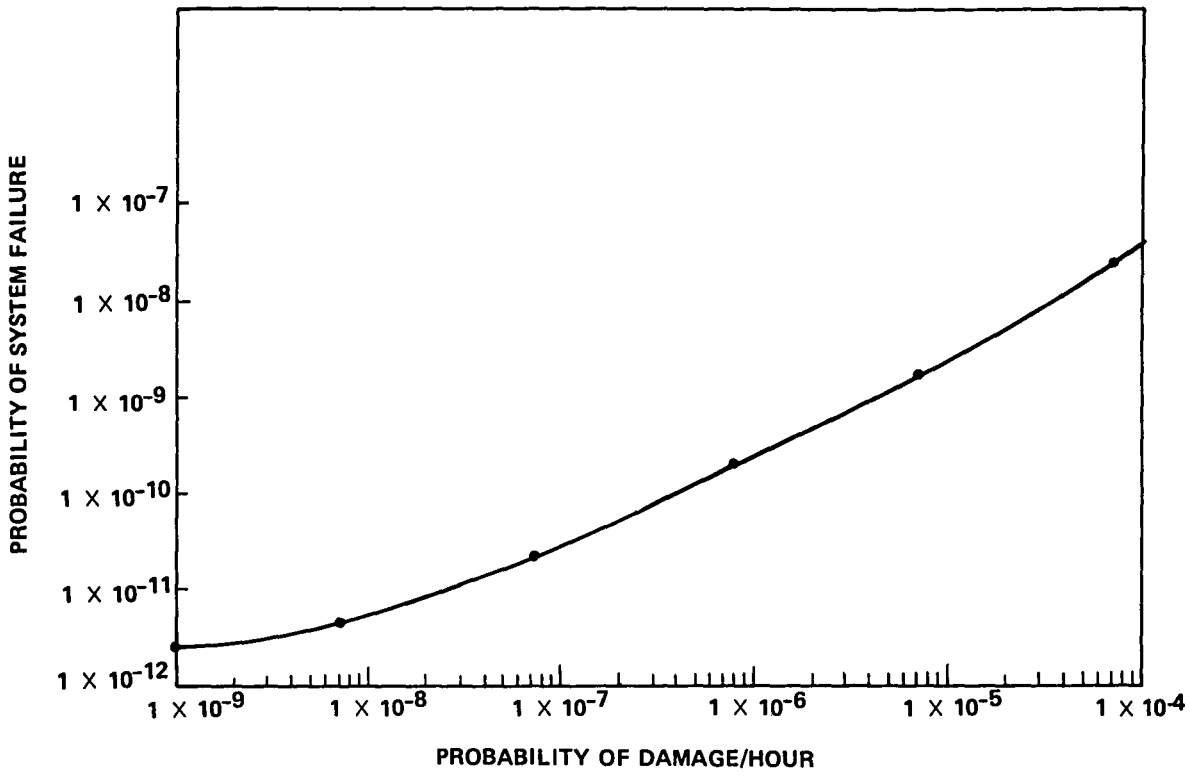

Figure 11. Probability of system failure vs. probability of damage for a separated IMU system.

Mission time and its effect on RSDIMU reliability was another parameter investigated. The results are presented in Figure 12. For realistic values of the probability of detection for a single FDI system channel, system reliability appears to be virtually independent of mission time in contrast to a system with perfect FDI.

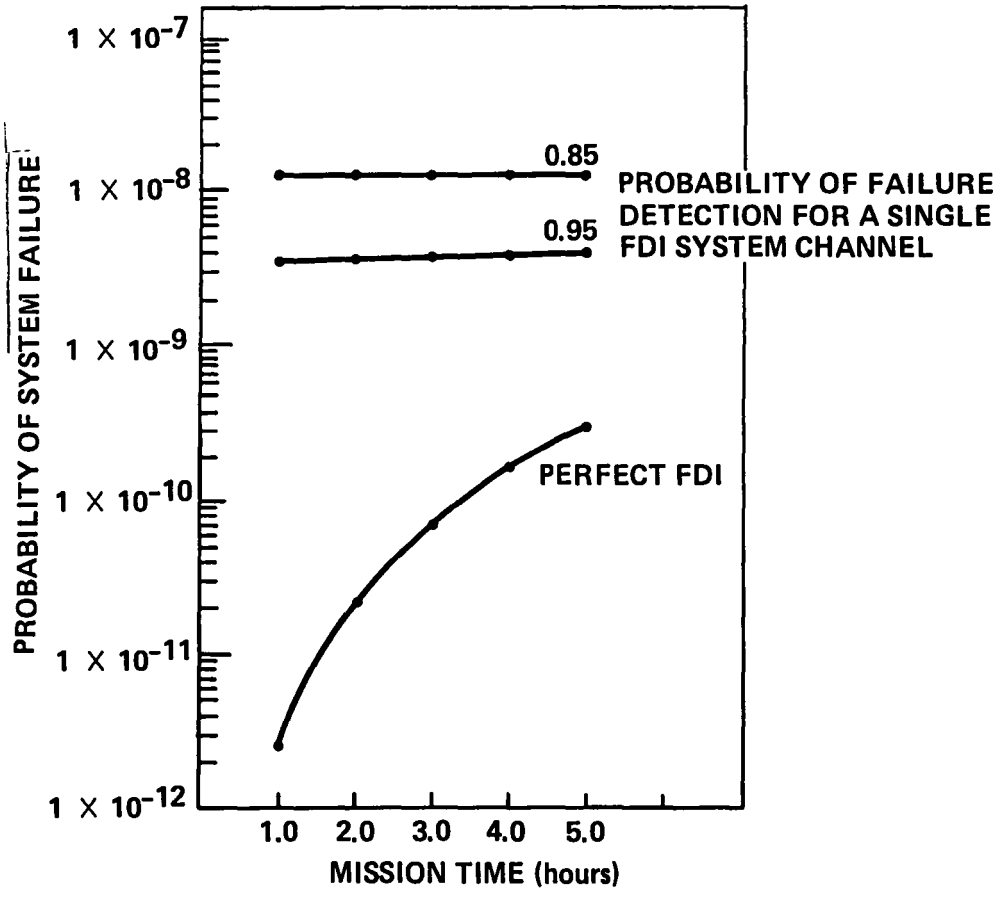

Figure 12. Probability of system failure vs. mission time.

The last effort undertaken in this area was to blend all of the results generated thus far to come up with an estimate of the reliability of a typical operational RSDIMU system. To do this, a gyro failure rate of $400/10^6$ hours (MTBF of 2000 hours) and an accelerometer failure rate of $333/10^6$ hours (MTBF of 3000 hours) were selected. These values were obtained from discussions with CSDL's Reliability and Quality Assurance Department. The thresholds were selected to be at 7.5σ and the probability of damage effects was assumed to be zero. A probability of soft-failure channel detection of 0.8 and a probability of correct soft-failure channel isolation of 0.99 were chosen. Use of these parameters resulted in a probability of system failures of 4.27×10^{-7} which is three orders

of magnitude better than that of the system with no FDI and redundancy management. This number is dictated by the probability of failure detection.

SECTION 4

DERIVATION OF DYNAMIC THRESHOLDS FOR THE DUAL, SEPARATED RSDIMU

4.1 Introduction

Reference 1 shows that some form of sensor uncertainty compensation is needed to detect soft failures with the RSDIMU system. The basic problem is that a dynamic flight environment excites the sensor uncertainties to a greater extent than during cruise. Therefore, if it is desired to detect as small a failure as possible when the vehicle is not maneuvering without encountering a prohibitive number of false alarms when the vehicle maneuvers, the environment must be compensated for in some fashion.

Dynamic thresholds were suggested as a solution to this problem during the previous CSDL program for NASA and a means for generating them developed. The work was restricted to the case where both halves of the RSDIMU are colocated. The thresholds consist of a constant and a dynamic portion. The constant accounts for high frequency effects such as quantization and sensor noise. The dynamic portion accounts for the effects of maneuvering flight on the sensor errors.

A block diagram depicting the method used to generate the dynamic thresholds is shown in Figure 13. The overall idea embodied in this methodology is to parallel the development of the failure decision function using an analytic expression for the worst-case sensor error. In Figure 13 the top path is one channel of the FDI system block diagram presented in Figure 3. The lower path describes the generation of the

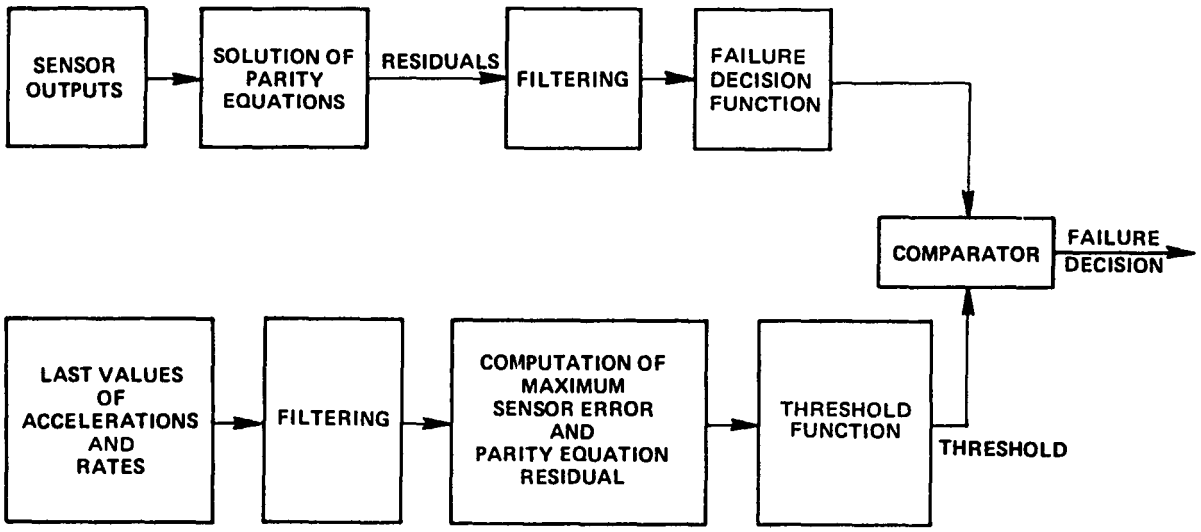

Figure 13. Generation of dynamic thresholds.

thresholds. The last values of the vehicle accelerations and rates obtained from the sensor outputs are filtered in the same way as the parity equation residuals. These quantities are then used to generate an upper bound for the parity equation residuals from an analytic expression. The threshold function is then generated in a manner corresponding to that in which the decision function is generated. The failure decision function and threshold are then compared to determine if a failure has occurred.

The concept of dynamic thresholds was evaluated via simulation to assess its feasibility, evaluate its effectiveness, and uncover any problems in applying it. A block diagram of the simulation used is shown in Figure 14. The core of the simulation is a six-degree-of-freedom aircraft model with nonlinear aerodynamics. Also modeled are a flight-control system and turbulence. An autopilot "commands" the vehicle to follow a desired trajectory profile. Skewed gyro and accelerometer sensor configurations are modeled with the location of the sensors variable to permit an assessment of accelerometer lever-arm effects. The sensors are assumed to be of navigation quality and used for navigation and

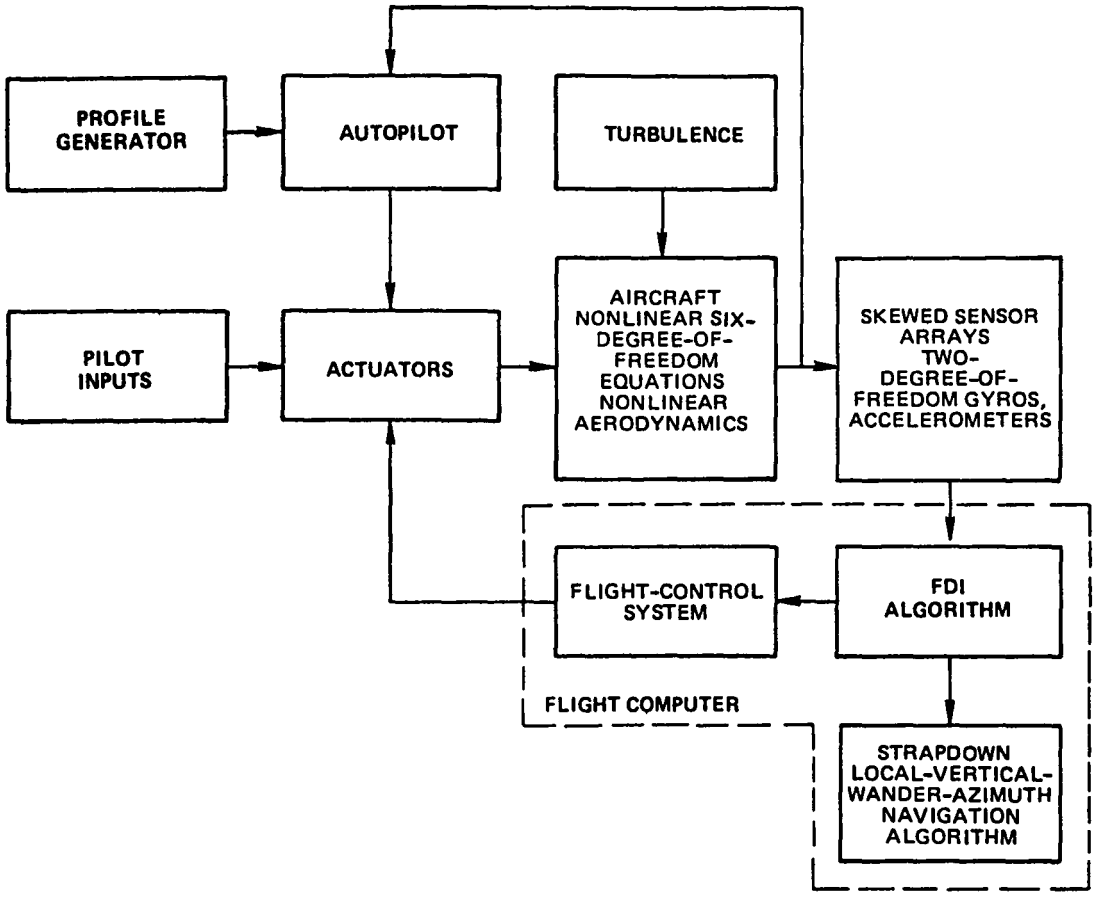

Figure 14. Simulation block diagram.

flight-control purposes. The FDI algorithm operates on the sensor data to generate the input signals to the flight-control and navigation systems. Navigation accuracy is assessed by differencing the outputs of a strapdown local-vertical-wander-azimuth navigation system model and the vehicle states.

Figure 15 shows the 1-hour flight profile used to evaluate the fault-tolerant system during the dynamic phases of the vehicle flight. The profile includes features from a typical transport aircraft mission profile: a climb to altitude, cruise, heading changes, descent, and a loiter maneuver.

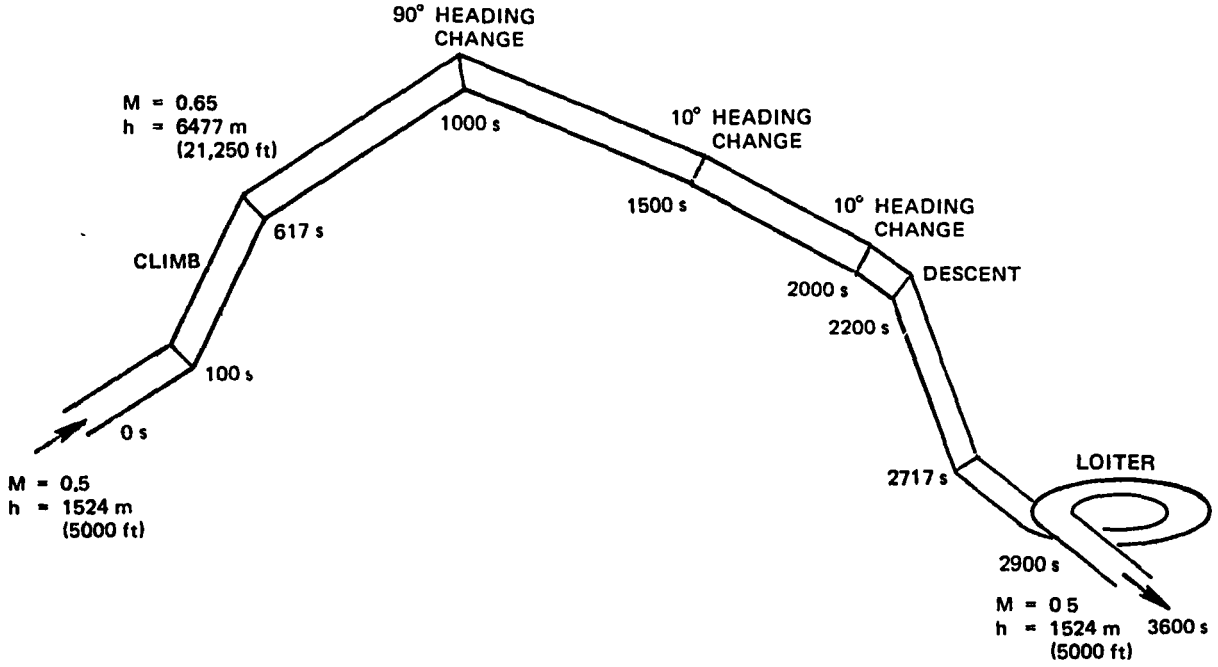

Figure 15. Evaluation trajectory profile.

The present program is concerned with the development and evaluation of an analytic technique for the generation of FDI thresholds for an aircraft system with dual, separated IMUs. The intent is to use all available instruments of both IMUs to detect and isolate sensor failures. The separation of the IMUs hinders failure detection and isolation, since the raw structural-mode and accelerometer lever-arm effects which the instruments sense are comparable in magnitude to the failures which may be encountered and can result in the false detection of failures if not properly accounted for. The selection of thresholds, a major consideration in the development of any FDI system, is especially complicated when separated, communicating IMUs are present, since these additional factors must be taken into account. A spectrum of failure magnitudes from hard through soft is considered. Finally, aircraft maneuvering adds a significant dimension to the problem and dictates the need for variable failure-detection thresholds to prevent the occurrence of false alarms.

4.2 Structural-Mode Effects

Each structural mode can be represented by a second-order differential equation with additional terms which, in general, couple in the basic rigid-body airframe response, the other modes, and the control-surface deflections. The effect of the structural modes on the angular rates and linear accelerations is a function of sensor location and is indicated by the following equations

$$p_B = p + \delta p_B = p + p_{\dot{\eta}_4}\dot{\eta}_4 + p_{\dot{\eta}_5}\dot{\eta}_5 + p_{\dot{\eta}_6}\dot{\eta}_6$$

$$q_B = q + \delta q_B = q + q_{\dot{\eta}_1}\dot{\eta}_1 + q_{\dot{\eta}_2}\dot{\eta}_2 + q_{\dot{\eta}_3}\dot{\eta}_3$$

$$r_B = r + \delta r_B = r + r_{\dot{\eta}_6}\dot{\eta}_6$$

$$n_{y_B} = n_y + \delta n_{y_B} = n_y + n_{y_{\ddot{\eta}_6}}\ddot{\eta}_6$$

$$n_{z_B} = n_z + \delta n_{z_B} = n_z + n_{z_{\ddot{\eta}_1}}\ddot{\eta}_1 + n_{z_{\ddot{\eta}_2}}\ddot{\eta}_2 + n_{z_{\ddot{\eta}_3}}\ddot{\eta}_3 \qquad (1)$$

4.3 Accelerometer Lever-Arm Effects

The linear accelerations measured at a distance d meters from the cg of the vehicle (in terms of the linear accelerations at the cg of the vehicle and the accelerometer lever-arm effects) are defined by the following equations

$$
\begin{aligned}
n_{x_d} &= n_{x_{cg}} + \delta n_{x_{\ell a}} \\
&= n_{x_{cg}} + \frac{1}{G_\phi} \\
&\quad \cdot \left[-(q^2 + r^2) d_x + (qp - \dot{r}) d_y + (\dot{q} + pr) d_z \right] \\
n_{y_d} &= n_{y_{cg}} + \delta n_{y_{\ell a}} \\
&= n_{y_{cg}} + \frac{1}{G_\phi} \\
&\quad \cdot \left[(\dot{r} + pq) d_x - (p^2 - r^2) d_y + (rq - \dot{p}) d_z \right] \\
n_{z_d} &= n_{z_{cg}} + \delta n_{z_{\ell a}} \\
&= n_{z_{cg}} + \frac{1}{G_\phi} \\
&\quad \cdot \left[(pr - \dot{q}) d_x + (qr - \dot{p}) d_y - (p^2 + q^2) d_z \right] \qquad (2)
\end{aligned}
$$

4.4 Background

The detection and isolation of the first two sensor failures and the detection of the third are required for the RSDIMU. Dynamic FDI system thresholds require an estimate of the incremental structural mode and accelerometer lever-arm effects between the locations of the two halves of the RSDIMU. References 4 and 5 describe a technique for generating these quantities which is satisfactory for the detection and isolation of the first sensor failure when the instruments are implemented in dual separated clusters. It uses the differences of the least-square estimates of the body-axes rates or acceleration from each half of the RSDIMU. This approach is valid only for the first failure because reconfiguration will

then leave only one instrument in one of the halves of the RSDIMU. The major contribution contained in this section of the report is the development of a technique for generating the incremental structural mode and accelerometer lever-arm effects which is valid for multiple, nonconcurrent instrument failures.

A concept for the least-square estimation of the structural mode and lever-arm effects which evolves from that presented in References 4 and 5 and which is applicable to multiple, nonconcurrent failures has been developed by Mr. F. Morrell of the NASA Langley Research Center. It uses least square estimates of all combinations of two valid instruments to obtain the desired information. Furthermore, it is rather simple in that the computation of only one component of the body axes rates or accelerations is required from the estimates obtained for each pair of sensors.

This section of the report describes a different approach to the problem using what is called a sensor-error estimation approach. Basically, the approach is to compute the least-square estimates of the body-axes rates or accelerations using one of the RSDIMU halves with unfailed instruments. Estimates of the instrument outputs for the other half of the RSDIMU are computed using the estimated body axes quantities and the nominal sensor geometry matrix. The actual and estimated sensor outputs are then differenced to produce estimates of the sensor uncertainties. Estimates of the structural mode and lever-arm effects are then generated by resolving the estimated sensor uncertainties through the FDI system parity equations. The absolute value of these estimated structural mode and lever-arm effects is then used as the worst case estimate for the thresholds.

The technique just described is derived for the EVT algorithm initially and later extended to the GLT. The accelerometers are considered rather than the gyros since both structural-mode and lever-arm effects must be considered. It is also assumed that filtering is present in the FDI channel being considered to indicate how this aspect of the system is treated.

4.5 EVT Parity Equations

The EVT parity equations are presented in this section. A complete derivation is included in Reference 1. The formulation is based on the projection of rates or accelerations measured in two planes along the line of intersection of the planes. As the measurement planes are orthogonal to the spin or pendulous axes, the "edge vectors" are defined by the line mutually perpendicular to these axes. They are the vectors, e_{ij}, defined in Figure 1. Rates or accelerations measured in the i and j planes may be compared if they are expressed in a common frame. The frame chosen here is the body frame. Then the residual R_{ij} may be expressed by

$$R_{ij} = (\omega_i^B - \omega_j^B) \cdot e_{ij}^B$$

If $|R_{ij}| > T$, an FDI threshold, then a miscompare flag, F_{ij}, is set. FDI consists of logical operations on the flags F_{ij}.

For the case under consideration, the accelerometer inputs are defined by the matrix equation

$$\begin{bmatrix} m_{a_{A1}} \\ m_{a_{B1}} \\ m_{a_{A2}} \\ m_{a_{B2}} \\ m_{a_{A3}} \\ m_{a_{B3}} \\ m_{a_{A4}} \\ m_{a_{B4}} \end{bmatrix} = \begin{bmatrix} \alpha & -\beta & \gamma \\ -\beta & \alpha & \gamma \\ \beta & \alpha & \gamma \\ -\alpha & -\beta & \gamma \\ -\alpha & \beta & \gamma \\ \beta & -\alpha & \gamma \\ -\beta & -\alpha & \gamma \\ \alpha & \beta & \gamma \end{bmatrix} \begin{bmatrix} n_x \\ n_y \\ n_z \end{bmatrix}$$

where

$$\alpha = \frac{\sqrt{3} - 1}{2\sqrt{3}}$$

$$\beta = \frac{\sqrt{3} + 1}{2\sqrt{3}}$$

$$\gamma = \frac{1}{\sqrt{3}}$$

The edge vector parity equations are

$$R_{12} = \frac{1}{\sqrt{2}} (\omega^B_{2y} - \omega^B_{1y} + \omega^B_{1z} - \omega^B_{2z})$$

$$R_{13} = \frac{1}{\sqrt{2}} (\omega^B_{1x} - \omega^B_{3x} + \omega^B_{3y} - \omega^B_{1y})$$

$$R_{14} = \frac{1}{\sqrt{2}} (\omega^B_{4x} - \omega^B_{1x} + \omega^B_{1z} - \omega^B_{4z})$$

$$R_{23} = \frac{1}{\sqrt{2}} (\omega^B_{2x} - \omega^B_{3x} + \omega^B_{2z} - \omega^B_{3z})$$

$$R_{24} = \frac{1}{\sqrt{2}} (\omega^B_{2x} - \omega^B_{4x} + \omega^B_{2y} - \omega^B_{4y})$$

$$R_{34} = \frac{1}{\sqrt{2}} (\omega^B_{3y} - \omega^B_{4y} + \omega^B_{3z} - \omega^B_{4z})$$

where the body axes accelerations for each instrument are

$$\omega^B_{1x} = \alpha m_{a_{A1}} - \beta m_{a_{B1}}$$

$$\omega^{B}_{1y} = -\beta m_{a_{A1}} + \alpha m_{a_{B1}}$$

$$\omega^{B}_{1z} = \gamma (m_{a_{A1}} + m_{a_{B1}})$$

$$\omega^{B}_{2x} = \beta m_{a_{A2}} - \alpha m_{a_{B2}}$$

$$\omega^{B}_{2y} = \alpha m_{a_{A2}} - \beta m_{a_{A2}}$$

$$\omega^{B}_{2z} = \gamma (m_{a_{A2}} + m_{a_{B2}})$$

$$\omega^{B}_{3x} = -\alpha m_{a_{A3}} + \beta m_{a_{B3}}$$

$$\omega^{B}_{3y} = \beta m_{a_{A3}} - \alpha m_{a_{B3}}$$

$$\omega^{B}_{3z} = \gamma (m_{a_{A3}} + m_{a_{B3}})$$

$$\omega^{B}_{4x} = -\beta m_{a_{A4}} + \alpha m_{a_{B4}}$$

$$\omega^{B}_{4y} = -\alpha m_{a_{A4}} + \beta m_{a_{B4}}$$

$$\omega^{B}_{4z} = \gamma (m_{a_{A4}} + m_{a_{B4}})$$

Combining the last two sets of equations results in the parity equations

$$R_{12} = \frac{1}{\sqrt{2}}\left[(\beta+\gamma)(m_{a_{A1}} - m_{a_{B2}}) + (\gamma-\alpha)(m_{a_{B1}} - m_{a_{A2}})\right]$$

$$R_{13} = \frac{1}{\sqrt{2}}\left[m_{a_{A1}} - m_{a_{B1}} + m_{a_{A3}} - m_{a_{B3}}\right]$$

$$R_{14} = \frac{1}{\sqrt{2}}\left[(\gamma-\alpha)(m_{a_{A1}} - m_{a_{B4}}) + (\gamma+\beta)(m_{a_{B1}} - m_{a_{A4}})\right]$$

$$R_{23} = \frac{1}{\sqrt{2}}\left[(\beta+\gamma)(m_{a_{A2}} - m_{a_{B3}}) + (\gamma-\alpha)(m_{a_{B2}} - m_{a_{A3}})\right]$$

$$R_{24} = \frac{1}{\sqrt{2}}\left[m_{a_{A2}} - m_{a_{B2}} + m_{a_{A4}} - m_{a_{B4}}\right]$$

$$R_{34} = \frac{1}{\sqrt{2}}\left[(\beta+\gamma)(m_{a_{A3}} - m_{a_{B4}}) + (\gamma-\alpha)(m_{a_{B3}} - m_{a_{A4}})\right] \qquad (3)$$

4.6 The Derivation of Dynamic Thresholds for the EVT

The basic approach is to start with an analytic expression for the sensor error, structural-mode, and lever-arm effects and obtain expressions for the parity-equation residuals. Upper bounds for the parity-equation residuals are then determined. The FDI system threshold is generated by duplicating the steps involved in the computation of the failure-decision function using the upper bounds for the parity-equation residuals rather than the actual residuals.

It is necessary to write expressions for the linear accelerations at one IMU location in terms of those at the others. Using the right half of the RSDIMU as a reference and Eq. (1) and (2) leads to the following results

$$n_{x_L} = n_{x_R} + \delta n_x$$

$$= n_{x_R} + \delta n_{x_{\ell a_L}} - \delta n_{x_{\ell a_R}}$$

$$n_{y_L} = n_{y_R} + \delta n_y$$

$$= n_{y_R} + \delta n_{y_{\ell a_L}} - \delta n_{y_{\ell a_R}} + \delta n_{y_{B_L}} - \delta n_{y_{B_R}}$$

$$n_{z_L} = n_{z_R} + \delta n_z$$

$$= n_{z_R} + \delta n_{z_{\ell a_L}} - \delta n_{z_{\ell a_R}} + \delta n_{z_{B_L}} - \delta n_{z_{B_R}}$$

The output of the j^{th} accelerometer of the right IMU can be written as

$$m_{a_j} = H_{j1} \cdot n_{x_R} + H_{j2} \cdot n_{y_R} + H_{j3} \cdot n_{z_R} + \delta m_{a_j}$$

$$j = A3, B3, A4, B4 \qquad (4)$$

δm_{a_j} is a term representing the sensor errors. The sensor models assumed for this study, described in detail in Reference 1, result in

$$\delta m_{a_j} = \lambda_j + (\mu_{j1} + \varepsilon_j \cdot H_{j1}) n_{x_R} + (\mu_{j2} + \varepsilon_j \cdot H_{j2}) n_{y_R}$$

$$+ (\mu_{j3} + \varepsilon_j \cdot H_{j3}) n_{z_R}$$

$$+ \alpha_{IP_j} (H_{j1} \cdot n_{x_R} + H_{j2} \cdot n_{y_R} + H_{j3} \cdot n_{z_R})$$

$$\cdot (H^p_{j1} \cdot n_{x_R} + H^p_{j2} \cdot n_{y_R} + H^p_{j3} \cdot n_{z_R})$$

$$+ \beta_{II_j} (H_{j1} \cdot n_{x_R} + H_{j2} \cdot n_{y_R} + H_{j3} \cdot n_{z_R})^2$$

$$j = A3, B3, A4, B4 \qquad (5)$$

A similar expression is obtained for the output of the k^{th} accelerometer of the left IMU using the appropriate accelerations. Use of the equations for the accelerations measured by the left half of the RSDIMU in terms of those of the right half leads to

$$m_{a_k} = H_{k1} \cdot n_{x_R} + H_{k2} \cdot n_{y_R} + H_{k3} \cdot n_{z_R}$$

$$+ \delta m_{a_k} + H_{k1} \cdot \delta n_x + H_{k2} \cdot \delta n_y + H_{k3} \cdot \delta n_z$$

$$k = A1, B1, A2, B2 \qquad (6)$$

Calculating the residuals from Eq. (3) results in

$$R_{12} = \frac{1}{\sqrt{2}} \left[(\beta + \gamma)(\delta m_{a_{A1}} - \delta m_{a_{B2}}) \right.$$

$$\left. + (\gamma - \alpha)(\delta m_{a_{B1}} - \delta m_{a_{A2}}) \right]$$

$$R_{13} = \frac{1}{\sqrt{2}} \left[\delta m_{a_{A1}} - \delta m_{a_{B1}} + \delta m_{a_{A3}} - \delta m_{a_{B3}} \right.$$

$$\left. + \delta n_x - \delta n_y \right]$$

$$R_{14} = \frac{1}{\sqrt{2}} \left[(\gamma - \alpha)(\delta m_{a_{A1}} - \delta m_{a_{B4}}) + (\gamma + \beta)(\delta m_{a_{B1}} - \delta m_{a_{A4}}) - \delta n_x + \delta n_z \right]$$

$$R_{23} = \frac{1}{\sqrt{2}} \left[(\beta + \gamma)(\delta m_{a_{A2}} - \delta m_{a_{B3}}) + (\gamma - \alpha)(\delta m_{a_{B2}} - \delta m_{a_{A3}}) + \delta n_x + \delta n_z \right]$$

$$R_{24} = \frac{1}{\sqrt{2}} \left[\delta m_{a_{A2}} - \delta m_{a_{B2}} + \delta m_{a_{A4}} - \delta m_{a_{B4}} + \delta n_x + \delta n_y \right]$$

$$R_{34} = \frac{1}{\sqrt{2}} \left[(\beta + \gamma)(\delta m_{a_{A3}} - \delta m_{a_{B4}}) + (\gamma - \alpha)(\delta m_{a_{B3}} - \delta m_{a_{A4}}) \right]$$

Several observations can be made from a consideration of the previous equations. First, the parity equation residuals are a function only of the uncertainties associated with the instruments. The parity equations remove the effects of the measured variables, i.e., accelerations or rates. Second, the parity equation residuals for the IMUs where the instruments are colocated, i.e., R_{12} and R_{34}, are not affected by the separation effects due to lever arms, bending and vibration as are the other parity equation residuals. If the left IMU is used as a reference, the same expressions for the residuals result with the exception that the signs of the δn_x, δn_y, and δn_z terms are reversed.

A set of dynamic thresholds can be obtained by determining an upper bound for each of the residuals. Performing a worst case analysis leads to

$$R_{12_m} = 2.45\ \delta m_{a_m}$$

$$R_{13_m} = 2.8284\ \delta m_{a_m} + \frac{1}{\sqrt{2}} \left| (\delta n_x - \delta n_y)_f \right|$$

$$R_{14_m} = 2.45\ \delta m_{a_m} + \frac{1}{\sqrt{2}} \left| (-\delta n_x + \delta n_z)_f \right|$$

$$R_{23_m} = 2.45\ \delta m_{a_m} + \frac{1}{\sqrt{2}} \left| (\delta n_x + \delta n_z)_f \right|$$

$$R_{24_m} = 2.8284\ \delta m_{a_m} + \frac{1}{\sqrt{2}} \left| (\delta n_x + \delta n_y)_f \right|$$

$$R_{34_m} = 2.45\ \delta m_{a_m} \qquad (7)$$

δm_{a_m} is an analytic expression for the upper bound of the sensor error effects. This expression is solved in real time using the following equation

$$\delta m_{a_m} = \left\{ \lambda_{a_m} + \mu_{a_m} (|n_{x_f}| + |n_{y_f}| + |n_{z_f}|) \right.$$
$$+ \varepsilon_{a_m} (|0.788675 n_{x_f}| + |0.788675 n_{y_f}| + |0.577350 n_{z_f}|)$$
$$\left. + (\beta_{II_m} + \alpha_{IP_m}) [(|0.788675 n_x| + |0.788675 n_y| + |0.577350 n_z|)^2]_f \right\} \qquad (8)$$

δm_{a_m} is obtained from Eq. (5) by assuming worst case conditions: the magnitude of H_{j1}, H_{j2}, H^P_{j1} and H^P_{j2} is less than or equal to 0.788675, and the sensor errors are additive and bounded by their 3σ values. Use is also made of the fact that $H_{j3} = 0.577350$. This is significant since the steady-state value of the maximum parity-equation residual governs the value of the soft failure detected with the FDI system. This steady-state value is governed by the instrument bias and the effect of the 1-g normal acceleration obtained during straight and level flight on the other sensor errors. This latter effect is influenced by the magnitude of H_{j3}. Thus, the use of the coefficient $H_{j3} = 0.577350$ will result in a lower threshold and the ability to detect smaller failures.

In the same manner, the angle of the accelerometer pendulous axis with respect to the x-y plane of the vehicle affects the level of soft failure detected through H^P_{j3} and the input-pendulous-axes coupling error. For this study, the accelerometers are mounted such that $H^P_{j3} = 0.577350$, i.e., at the same angle with respect to the x-y plane as the input axes of the instruments.

R_{13_m}, R_{14_m}, R_{23_m}, and R_{24_m} each contain a term which reflects the incremental value of the separation effects between the two IMU locations. If three or more independent measurements are available at each IMU location, the required quantitites can be obtained by generating a least-squares solution for n_x, n_y, and n_z at each IMU location and differencing like quantities. This approach falls apart after the first failure is detected and isolated since one instrument is analytically removed from the system. Therefore, a least-squares solution can be obtained for only one IMU.

A technique has been developed for generating the incremental separation effects which overcomes the deficiencies of the approach described in the previous paragraph. The least-squares solution of only one of the IMUs is required. Assume for the purposes of discussion that the right IMU is selected as the reference. This is a minor restriction which will be removed later. A least-squares solution can be obtained

for the right IMU resulting in the estimated quantites $\hat{n}_{x_R}$, $\hat{n}_{y_R}$, and $\hat{n}_{z_R}$. An estimate of the separation effects on the instruments of the left IMU can be obtained by using $\hat{n}_{x_R}$, $\hat{n}_{y_R}$, and $\hat{n}_{z_R}$ to generate an estimate of the measurements of the left IMU and subtracting them from the actual measurements. For example

$$\hat{m}_{a_{A1}} = \alpha\hat{n}_{x_R} - \beta\hat{n}_{y_R} + \gamma\hat{n}_{z_R}$$

$$\begin{aligned}\delta\hat{m}_{a_{A1}} &= m_{a_{A1}} - \hat{m}_{a_{A1}} \\ &= \alpha(n_{x_L} - \hat{n}_{x_R}) - \beta(n_{y_L} - \hat{n}_{y_R}) + \gamma(n_{z_L} - \hat{n}_{z_R}) \\ &= \alpha\delta\hat{n}_x - \beta\delta\hat{n}_y + \gamma\delta\hat{n}_z \end{aligned} \quad (9)$$

Following this procedure leads to

$$\begin{aligned}\delta\hat{m}_{a_{B1}} &= -\beta\delta\hat{n}_x + \alpha\delta\hat{n}_y + \gamma\delta\hat{n}_z \\ \delta\hat{m}_{a_{A2}} &= \beta\delta\hat{n}_x + \alpha\delta\hat{n}_y + \gamma\delta\hat{n}_z \\ \delta\hat{m}_{a_{B2}} &= -\alpha\delta\hat{n}_x - \beta\delta\hat{n}_y + \gamma\delta\hat{n}_z \end{aligned} \quad (10)$$

Since the right IMU is the reference

$$\delta\hat{m}_{a_{A3}} = 0$$

$$\delta\hat{m}_{a_{B3}} = 0$$

$$\delta\hat{m}_{a_{A4}} = 0$$

$$\delta\hat{m}_{a_{B4}} = 0 \qquad (11)$$

Consider the parity equation R_{13}. Any uncertainty in the measurements from instruments 1 and 3 is reflected in R_{13} according to the equation

$$\delta\hat{R}_{13} = \frac{1}{\sqrt{2}}\left[\delta\hat{m}_{a_{A1}} - \delta\hat{m}_{a_{B1}} + \delta\hat{m}_{a_{A3}} - \delta\hat{m}_{a_{B3}}\right] \qquad (12)$$

Substituting Eq. (9), (10), and (11) into Eq. (12) leads to

$$\delta\hat{R}_{13} = \frac{1}{\sqrt{2}}\left[\delta\hat{n}_x - \delta\hat{n}_y\right]$$

which is an estimate of the quantity needed for the threshold.

Thus, the procedure for generating an estimate of the effects of the IMU separation for the thresholds is to generate a least-squares solution for the accelerations of one of the IMUs of the system. These estimates are then used to form an estimate of the measurements of the other IMU. The estimated measurements are subtracted from the true

measurements to obtain the estimated effects of the separation on the measurements. The quantities needed for the thresholds are then obtained by resolving these uncertainties through the parity equations. The absolute value of the solution is used for the thresholds.

Several additional items regarding the thresholds should be pointed out at this time. One is that the last value of the linear accelerations (generated for the flight-control system from the sensor signals) can be used to generate the thresholds. Using these signals results in thresholds which reflect the current state of the aircraft and its environment.

The effect of the filtering present in the mid- and soft-failure channels on the generation of the thresholds is now considered. In order to make a valid comparison between the residuals and thresholds, it is necessary to filter each in an identical fashion. It is preferable to filter the quantities required for the thresholds before the maximization and absolute values are generated. This results in a reduced level of noise which is not subject to maximization and leads to lower, more realistic thresholds.

The subscript f in Eq. (7) and (8) indicates where the filtering should occur in the generation of the thresholds. When n_x, n_y, and n_z linearly affect the parity-equation residuals, it is possible to interchange the operations of addition and multiplication by a constant and filtering. It is not valid to do this with the nonlinear, input-axes-squared, and input-pendulous-axes-coupling errors, however. The nonlinear quantity must be formed and then filtered.

A development corresponding to the one undertaken with the right IMU as the reference can be generated using the left IMU as the reference. The same expressions for the thresholds as presented in Eq. (7) are obtained. For this case

$$\delta\hat{m}_{a_{A1}} = \delta\hat{m}_{a_{B1}} = \delta\hat{m}_{a_{A2}} = \delta\hat{m}_{a_{B2}} = 0.0$$

Nonzero estimates for the separation effects on instruments 3 and 4 result which are

$$\delta\hat{m}_{a_{A3}} = -\alpha\delta\hat{n}_x + \beta\delta\hat{n}_y + \gamma\delta\hat{n}_z$$

$$\delta\hat{m}_{a_{B3}} = \beta\delta\hat{n}_x - \alpha\delta\hat{n}_y + \gamma\delta\hat{n}_z$$

$$\delta\hat{m}_{a_{A4}} = -\beta\delta\hat{n}_x - \alpha\delta\hat{n}_y + \gamma\delta\hat{n}_z$$

$$\delta\hat{m}_{a_{B4}} = \alpha\delta\hat{n}_x + \beta\delta\hat{n}_y + \gamma\delta\hat{n}_z$$

The effects of these quantities on the residuals are of the same magnitude but opposite in sign to those obtained previously. Thus the same thresholds result.

It is necessary to examine the effect of failures on the thresholds. The statistics of the parity equation residuals change to reflect the presence of a failure, e.g., the mean changes due to a bias failure. If one of the instruments of the reference IMU fails, the least-square estimate of the accelerations or rates will change to reflect the presence of this failure. This failure will in turn affect the thresholds via the terms generated to account for the separation effects. Similarly if the failure occurs in one of the instruments not in the reference IMU, the instrument output used to generate the separation effects will reflect the failure and result in a change in the threshold. As things presently stand, both the residuals and thresholds change due to a failure and detection and isolation is not possible. Modifications must be made to the FDI algorithm to eliminate this deficiency.

The technique employed is to pass the estimated separation effects through washout filters before taking the absolute value for the thresholds. These filters have the effect of attenuating the low-frequency data of the signals while passing the high-frequency data intact. Washout filtering removes the effect of the instrument biases and bias failures from the separation effects so that the thresholds return to their prefailure values. The parity equation residuals change to reflect the effect of the failures and failure detection and isolation occurs when the thresholds are exceeded.

The approach defined in the previous paragraph will also work properly for nonbias-type failures. The washout filter has a differentiating effect on the separation effects so that the residuals change as a function of the integral of the effect on the thresholds. For example, consider a ramp failure. The residuals will change linearly with time while the thresholds will change by a constant amount.

It is not necessary to washout filter the portion of the FDI thresholds due to the sensor errors. This is true since any error effect in the least-squares estimate of the accelerations is modified by the 3σ value of a sensor error which reduces its effect to second order.

The FDI algorithm just developed offers several possibilities for implementation. The most conservative approach but also the most demanding in terms of computational requirements would involve the implementation of two identical FDI algorithms, one using each IMU as a reference. This scheme affords dual detection capability for the first failure, a feature which would lower the false alarm rate. The algorithm associated with the IMU containing unfailed instruments could then be used for the detection and isolation of the second and third failures.

The FDI algorithm proposed accounts for factors such as the detection and isolation of soft instrument failures, the effects of vehicle dynamics, and IMU separation. It is valid as long as the basic assumptions upon which the thresholds are derived are valid. One instance where this may not be true is when saturation-type failures occur for which the instrument outputs do not contain information about the separation effects. If the failure is large enough, it will be detected and isolated via the hard-failure channel and the system reconfigured to eliminate its effect before the instrument output is used. The shorting of an instrument output is an example of this type of failure. It is equivalent to a failure of a large magnitude and is detected via the hard-failure channel on the first subsequent pass of the FDI algorithm. Built-in test equipment (BITE) would also be valuable in detecting and isolating failures of this nature and should be an integral part of the final FDI system.

4.7 Description of the GLT Algorithm

The GLT algorithm is briefly described in this section. Consider first the hard-failure channel. In the absence of sensor failures, the measurement equation is

$$m = H\omega + \zeta \tag{13}$$

A set of parity equations is defined by

$$\rho = Vm \tag{14}$$

where

$$VH = 0$$

V is assumed to be of dimension $(n - 3) \times n$. The matrix V can be chosen so that

$$VV^T = I$$

Substituting Eq. (13) into Eq. (14) yields

$$\rho_N = V\zeta$$

In the absence of sensor failures, ρ_N depends only on the measurement noise. If sensor j experiences a bias-type failure and that failure is manifest as an apparent bias shift of magnitude b in measurement j, then

$$\rho_F = V\zeta + V_j b$$

The difference in the statistics of ρ_N (in the absence of failures) and ρ_F (in the presence of failures) provides a basis for detecting and isolating failures. The problems of detecting and isolating sensor failures fall within the general framework of composite hypothesis tests, since the sign as well as the magnitude of the bias failure is unknown a priori.

A GLT formation of the detection and isolation problems has been developed. Assume single-axis failures initially. The GLT decision functions for detection and isolation are

$$DF_D = \rho^T\rho$$

$$DF_{I_j} = \frac{\left(\rho^T V_j\right)^2}{V_j^T V_j}, \quad j = 1,2,\ldots,n \tag{15}$$

These decision functions are strictly functions of the parity-equation residuals, ρ. The detection decision is made by comparing DF_D (which is

the sum of the squares of the parity-equation residuals) to a detection threshold. A sensor failure results in a change in the mean value of a sensor output, the parity-equation residuals, and the failure-detection function. The isolation decision is then made by determining $\max_j(DF_{I_J})$. The value of j that maximizes DF_{I_J} identifies the sensor that is most likely to have failed.

The preceding discussion assumes a set of n SDOF instruments. The extension to TDOF sensors requires certain modifications to reflect the characteristics of these instruments. Correlation between the noise present in the two measurements derived from a TDOF sensor is possible. One approach is to assume no correlation, design the FDI algorithms accordingly, and examine the degradation of FDI performance which occurs due to the presence of the nonzero values of correlation. This approach leads to the simplest algorithms and is preferred when the performance penalty incurred for nonzero values of correlation is acceptably small. In this case, the detection problem formulation is not changed, and the appropriate decision function is given by Eq. (15).

In formulating the isolation problem, another characteristic of TDOF sensors must be considered. A TDOF sensor failure may be reflected in either or both of its measurement axes. In practice, a failure observed in either axis is sufficient to disqualify the data from both of the sensor axes. Thus, isolation of a failed sensor rather than of a failed axis is sufficient. The isolation problem then involves testing only n/2 hypotheses. The GLT decision function for isolation which corresponds to Eq. (15) is

$$DF_{I_J} = \rho^T V_J (V_j^T V_J)^{-1} V_J^T \rho \qquad j = 1,2,\ldots,n/2$$

where $V_J = [V_{2j-1}, V_{2J}]$ and V_{2j-1}, V_{2J} are the two columns of the V matrix associated with TDOF sensor j.

The detection and isolation of the mid and soft failures is accomplished using the same decision functions as for the hard-failure channel. The only exception is that the appropriately filtered parity-equation residuals are used in lieu of the unfiltered ones.

4.8 The Derivation of Dynamic Thresholds for the GLT

The same general approach used to generate the dynamic thresholds in the case of the EVT applies to the GLT. Assume that the right half of the RSDIMU is the reference. Substituting Eq. (4) and (6) into the parity equations results in the following residuals

$$\rho_i = \sum_j V_{ij}\,\delta m_{a_j} + \sum_k V_{ik}(H_{ki}\delta n_x + H_{k2}\delta n_y + H_{k3}\delta n_z)$$

$$i = 1,2,\ldots,n-3;\ j = A1,B1,\ldots,A4,B4;\ k = A1,B1,A2,B2 \tag{16}$$

This expression results since VH = 0. It consists of two terms. The first results from the sensor errors and the second from the incremental structural mode and lever-arm effects between the locations of the two halves of the RSDIMU.

An upper bound for Eq. (16) is

$$\rho_{i_m} = \left(\sum_j |V_{ij}|\right)\delta m_{a_m} + \left|\sum_k V_{ik}(H_{k1}\delta n_x + H_{k2}\delta n_y + H_{k3}\delta n_z)\right|$$

$$i = 1,2,\ldots,n-3;\ j = A1,B1,\ldots,A4,B4;\ k = A1,B1,A2,B2 \tag{17}$$

The dynamic threshold is then obtained by summing the squares of the upper bound for each parity equation, i.e., duplicating the generation of the decision function. The resulting expression is

$$T = \sum_{i=1}^{n-3} (\rho_{1_m})^2 \qquad (18)$$

In order to calculate the FDI system thresholds, Eq. (18), and hence Eq. (17), must be calculated in real time. Consider the first term of Eq. (17). The V_{ij}'s are known and δm_{a_m} is the upper bound for the sensor errors given by Eq. (8). The only terms that have to be determined are the incremental effects of the structural modes and lever arms, i.e., the $(H_{k1}\delta n_x + H_{k2}\delta n_y + H_{k3}\delta n_z)$ terms. They may be generated by using the sensor error estimation approach described for the EVT. The derivation of Eq. (9), (10), and (11) demonstrate the method.

Many comments were made during the development of the dynamic thresholds for the EVT approach regarding their implementation, the low-pass filtering and washout filter, for example. All of these comments apply to the GLT approach as well but are not repeated here for brevity.

4.9 Simulation Validation and Results

Both the least-square and sensor-error techniques for estimating the structural-mode and lever-arm effects have been programmed into the CSDL simulation described in Section 4.1 to validate the concepts and uncover any additional problems which may exist with regard to their implementation.

An example of the results obtained is shown in Figure 16 and Table 5. These results were obtained using the GLT algorithm with three soft accelerometer failures introduced into the aircraft system flying the trajectory presented in Figure 15. Table 5 indicates when the failures were introduced, their magnitudes, the failed axis and the time at which the failures were detected. The time histories presented in Figure 16 show the hard-, mid-, and soft-failure decisions functions obtained during the one-hour flight and the soft-failure channel threshold implemented via Eq. (18). Consider first the failure decision functions. The

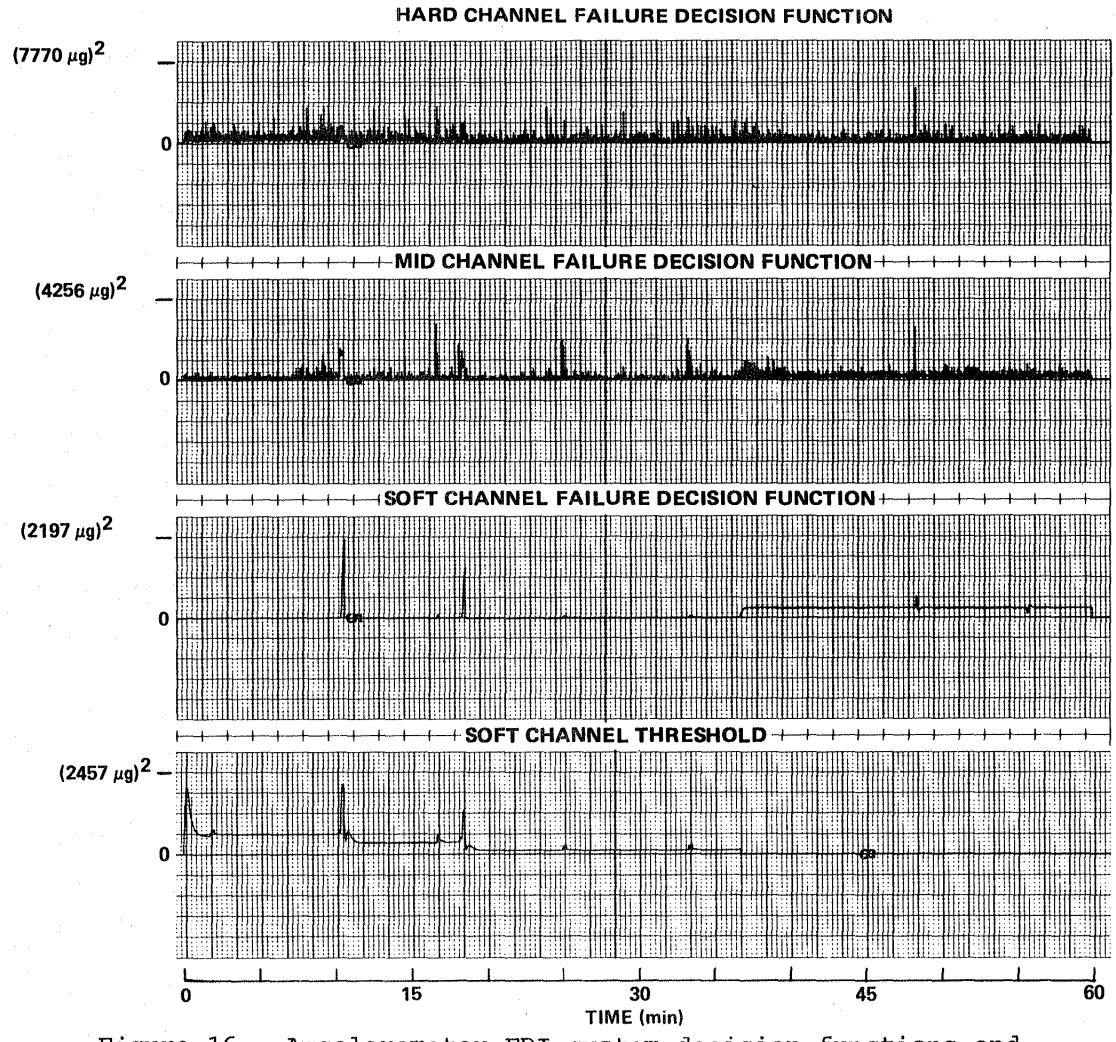

Figure 16. Accelerometer FDI system decision functions and soft-channel threshold decision functions.

Table 5. Simulation example data.

Time of Failure Input	Magnitude of Failure	Axis	Detection Time
sec	μg		sec
617	3000	B2	633.48
1100	3000	B3	1113.98
2200	4000	B4	2209.98

hard-failure channel decision function response is characterized by quantization noise. Its magnitude of $(7770\ \mu g)^2$ set a lower bound on the magnitude of failure which can be detected reliably with this channel without false alarms. The effect of low-pass filtering to enhance the detectability of smaller failures is evident from the mid- and soft-failure channel decision functions. The effect of the three failures is clearly evident in the soft-failure channel decision function. The first two spikes are caused by the introduction of the first two failures into the system and the elimination of their effects by reconfiguration. The third failure is evident as a step response in the soft-failure decision function since the failure can only be detected and not isolated. The effect of vehicle maneuvers are also evident, e.g., the spikes superimposed on the step effect due to the third failure. These are caused by the loiter maneuver.

The soft-failure channel threshold is also shown in Figure 16. An initial engage transient is present in this response along with spikes due to the first two sensor failures. The washout filter in the threshold generation algorithm causes the thresholds to return to their pre-failure values, resulting in failure detection. After each of the first two failures are detected and the system reconfigured, a lower threshold results since fewer parity equations are required for detection and isolation. With the detection of the third failure, the thresholds are set to zero in the algorithm. Maneuver effects are also evident in the threshold.

The results of the simulation tend to confirm the validity of the sensor-error and least-square estimation techniques for generating estimates of the incremental structural mode and lever-arm effects for dynamic thresholds. Multiple, nonconcurrent failures have been detected and isolated using both concepts. However, it is cautioned that only a limited number of evaluations have been made and further refinements to the algorithm may result from more extensive testing.

SECTION 5

SUMMARY

Two major goals were achieved during the course of this program. The first was the development and application of a technique for quantitatively evaluating the reliability of the RSDIMU. A detailed development of the Markov model generated for this purpose was presented. The results of the study of the impact of pertinent system parameters on the reliability of the RSDIMU were discussed. Many significant conclusions were drawn from these results. For example, the impact of false alarms on system reliability was one of those discussed in Section 3.1.

The second major goal achieved during this program was the development of an algorithm for generating dynamic thresholds for the dual, separated RSDIMU which is valid for the detection of multiple, nonconcurrent failures. It takes into account the incremental effects of the structural modes and accelerometer lever arms between the two sensor locations which are a significant factor. A technique called the sensor-error method of estimating these quantities was presented. In addition to an analytic development of this algorithm, the results of its evaluation via simulation are presented and discussed.

LIST OF REFERENCES

1. Motyka, P., et al., Failure Detection and Isolation Analysis of a Redundant Strapdown Inertial Measurement Unit, NASA Contractor Report 165658, February 1981.

2. Craig, R.J., and J. Russell, "Failure Modes and Redundancy Analysis for the Multifunction Inertial Reference Assembly (MIRA)," AFFDL-TR-78-25, March 1978.

3. Gai, E., J. Harrison, and K. Daly, "FDI Performance of Two Redundant Sensor Configurations," IEEE Transactions on Aerospace and Electronic Systems, Vol. AES-15, No. 3, May 1979.

4. Motyka, P., "A Failure Detection and Isolation System for Tactical Aircraft with Separated IMUs," Proceedings of NAECON '81, May 1981.

5. Motyka, P., "Fault Detection for Two Physically Separated, Communicating Inertial Measurement Units," 1981 Joint Automatic Control Conference, Charlottesville, VA, June 1981.

TECHNICAL REPORT STANDARD TITLE PAGE

1. Report No.	2. Government Accession No.	3. Recipient's Catalog No.
NASA CR-166050		

4. Title and Subtitle	5. Report Date
RELIABILITY ANALYSIS AND FAULT-TOLERANT SYSTEM DEVELOPMENT FOR A REDUNDANT STRAPDOWN INERTIAL MEASUREMENT UNIT	March 1983
	6. Performing Organization Code
7. Author(s)	8. Performing Organization Report No.
P. Motyka	CSDL-R-1588
9. Performing Organization Name and Address	10. Work Unit No.
The Charles Stark Draper Laboratory, Inc. 555 Technology Square Cambridge, Massachusetts 02139	11. Contract or Grant No. NAS1-16887
	13. Type of Report and Period Covered Final Report November 1981-November 1982
12. Sponsoring Agency Name and Address National Aeronautics and Space Administration Washington, D.C. 20546	14. Sponsoring Agency Code

15. Supplementary Notes

Langley Technical Monitor: Frederick R. Morrell

16. Abstract

A methodology is developed and applied for quantitatively analyzing the reliability of a dual, fail-operational redundant strapdown inertial measurement unit (RSDIMU). The RSDIMU consists of four two-degree-of-freedom gyros and accelerometers mounted on the faces of a semi-octahedron which can be separated into two halves for damage protection. A Markov evaluation model is defined in terms of the operational states of the RSDIMU to predict system reliability. A 27-state model is defined based upon a candidate redundancy management system which can detect and isolate a spectrum of failure magnitudes. The results of parametric studies are presented which show the effect on reliability of the gyro failure rate, both the gyro and accelerometer failure rates together, false alarms, probability of failure detection, probability of failure isolation, and probability of damage effects and mission time.

A technique is developed and evaluated for generating dynamic thresholds for detecting and isolating failures of the dual, separated IMU. The thresholds account for sensor error, structural mode, and accelerometer lever-arm effects. Special emphasis is given to the detection of multiple, nonconcurrent failures. Digital simulation time histories are presented which show the thresholds obtained and their effectiveness in detecting and isolating sensor failures.

17. Key Words Suggested by Author	18. Distribution Statement
Failure Detection and Isolation Redundant Inertial Measurement Unit Reliability Analysis	Unclassified - Unlimited

19. Security Classif. (of this report)	20. Security Classif. (of this page)	21. No. of Pages	22. Price
Unclassified	Unclassified		

End of Document